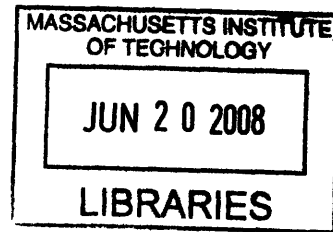


A Novel Polymeric Microelectrode Array for Highly Parallel, Long-Term
Neuronal Culture and Stimulation.

by

Giovanni Talei Franzesi

B.S. in Mechanical Engineering-Biomedical Engineering Track
Massachusetts Institute of Technology, 2006



Submitted to the Harvard-MIT Division of Health Sciences and Technology in partial
fulfillment of the requirements for the degree of

MASTER OF ENGINEERING IN BIOMEDICAL ENGINEERING

ARCHIVES

February 2008

© 2008 Massachusetts Institute of Technology. All rights reserved.

Signature of Author _____
Harvard-MIT Division of Health Sciences and Technology

Certified by _____
Martha Constantine-Paton
Professor of Biology and Brain and Cognitive Sciences,
Investigator, McGovern Institute

Certified by _____
Ian W. Hunter
Hatsopoulos Professor of Mechanical Engineering,
Director, BioInstrumentation Laboratory

Accepted by _____
Martha Gray
Director, Division of Health Sciences and Technology,
Professor of Electrical and Medical Engineering

A Novel Polymeric Microelectrode Array for Highly Parallel, Long-Term Neuronal Culture and Stimulation.

by

Giovanni Talei Franzesi

Submitted to the Harvard-MIT Division of Health Sciences and Technology in partial fulfillment of the requirements for the degree of

MASTER OF ENGINEERING IN BIOMEDICAL ENGINEERING

February 2008

ABSTRACT

Cell-based high-throughput screening is emerging as a disruptive technology in drug discovery; however, massively parallel electrical assaying of neurons and cardiomyocytes has until now been prohibitively expensive.

To address this limitation, we developed a scalable, all-organic 3D microelectrode array technology. The cheap, disposable arrays would be integrated into a fixed stimulation and imaging setup, potentially amenable to automated handling and data analysis. A combination of activity-dependent plasticity, made possible by independent control of up to 64 stimulating electrodes, and, eventually, of substrate chemical patterning would be employed to constrain the neuronal culture network connectivity. In order to ensure long-term survival of the cultures, a bottom feeder layer of glial cells would be grown.

In addition to high-throughput screening application, the polymeric microelectrode arrays and integrated stimulation systems were designed to allow the long-term study of synaptic plasticity, combining excellent long-term culture capabilities with a unique ability to independently control each electrode stimulation pattern. The resulting activity could be monitored optically, e.g, with calcium or voltage sensitive dyes, and the images could be stored and processed (possibly even in real time) within the same environment (LabView) as the stimulator.

To fabricate the polymeric microelectrode array, we prepare a multilayered mask substrate, by reversibly bonding together two sheets of implant-grade polydimethylsiloxane (PDMS) sheets, with or without a glass coverslip between them. Thanks to PDMS self-adhesive properties the various layers are held together stably but reversibly. The mask is then laser-patterned, using either a standard CO₂ laser or a 193 nm excimer laser. The mask can then be adhered onto a glassy carbon or ITO electrode, and polypyrrole, doped with either hyaluronic acid or sodium dodecylbenzenesulfonic acid, can be electrodeposited through it. Finally, the construct is removed from the deposition bath and the upper, sacrificial mask layer carefully peeled away. This fabrication method

allows exquisite control overall 3D electrode geometry, is suitable to produce structures between one and several hundred micrometers in diameter, either filled or tubular, and scales extremely well, so that, for example, 384 by 64 electrodes arrays can be patterned in just a few minutes and grown in the same time as a single array.

Thesis supervisor: Martha Constantine-Paton

Title: Professor of Biology and Brain and Cognitive Sciences, Investigator, McGovern Institute

Thesis supervisor: Ian W. Hunter

Title: Hatsopoulos Professor of Mechanical Engineering, Director, BioInstrumentation Laboratory

ACKNOWLEDGEMENTS

Many people, both in the Bioinstrumentation Laboratory and at the McGovern Institute, have helped make this work possible.

Special thanks must go to Dr. Andrew Taberner, who worked closely with me throughout the ups and downs of the project, helping me with a variety of issues and providing invaluable feedback.

Within the Bioinstrumentation Laboratory, I was also very lucky to have the help, in the form of training and discussions from Patrick Anquetil, Ph.D, Priam Pillai, Nathan Wiedenman, Craig Forest, Ph.D, Tim Fofonoff, and Cathy Hogan, Ph.D.

In the Constantine-Paton Laboratory, I must similarly thank Margaret Threadgill, Ph.D, Yasunobu Murata, M.D., and Akira Yoshii, Ph.D. for their time and kindness, in particular in helping me with neuronal cell culture.

This work was jointly supported by the Bioinstrumentation Laboratory and the McGovern Institute Neurotechnology (MINT) Program. I must thank McGovern Institute Director, Professor Robert Desimone, and MINT director, Dr. Charles Jennings for having believed in the project from the very beginning and for having been instrumental in making it possible.

Finally, I must thank Professors Ian W. Hunter and Martha Constantine-Paton for having offered me this opportunity and, throughout my work, having given invaluable guidance as well as having been truly inspiring mentors.

TABLE OF CONTENTS

1. INTRODUCTION

1.1 Current MEA technology

1.2 Our approach

1.3 High-throughput cell-based drug screening

1.4 Neuronal plasticity

1.5 Spike timing dependent neuronal plasticity (STDP)

1.6 Conductive polymers

1.7 Polypyrrole in biotechnology

2. ELECTRODE STIMULATOR

2.1 All-channel stimulator

2.2 64-channel, integrated stimulator

2.3 Interface and testing

2.4 Electrode substrate

3. PMEA

3.1 Fundamental constraints: biocompatibility and amenability to mass fabrication

3.2 Polypyrrole micropillar fabrication techniques

3.2.1 Free growth on EDM'd array

3.2.2 Free growth on planar MEAs

3.2.3 Interstitial deposition, PPy-PDMS nanocomposites

3.2.4 Electrodeposition through a mask

3.2.4.1 Mask fabrication techniques

Molding

Punching

Laser patterning

3.2.4.2 PPy electrodeposition

3.2.4.3 Mask surface layer removal

Etching

Peeling

3.2.5 Current fabrication workflow

3.2.6 Testing

3.2.7 Compatibility with standard cell-culture/high throughput formats

4. CONCLUSIONS

4.1 What has been accomplished to date

4.2 Next steps for the PME A technology

4.3 Applications

APPENDIX 1: Culture Protocol for CA3-CA1 neurons

From Margaret E Threadgill, PhD

APPENDIX 2: Protocol for PME A fabrication

REFERENCES

1. INTRODUCTION

The overall goal of the, ongoing, project is to develop a three-dimensional microelectrode array (MEA) for neuronal culture, with associated stimulation and imaging system, to be used both for high-throughput cell-based drug screening and for investigation of spike-timing-dependent-plasticity in dissociated neuronal cultures. In this thesis we describe the fabrication technologies explored and developed for the fabrication of the polymeric microelectrode array (PMEA), as well as the electrical stimulation and interface system.

1.1 Current MEA technology

Although micro electrode arrays for stimulation and recording of neuronal activity are currently commercially available (e.g. <http://www.multichannelsystems.com>), the flat topography limits effective cell-electrode contact. Moreover, while it is important for maintaining long-term culture viability to have a feeder layer of glial cells, this presents problems with current electrode designs: in order to effectively stimulate the overlying neurons a very high current must be applied, damaging the glial cells. By creating an extra layer between the electrodes and the neurons, glial cells also effectively increase the recording impedance, degrading the quality of electrical recordings from the overlying neurons.

Moreover, current systems, while allowing simultaneous recording from all the electrodes in the array not used for stimulation, can use just a few electrodes for stimulation, and even that at the cost of considerable artifacts in the electrical recordings.

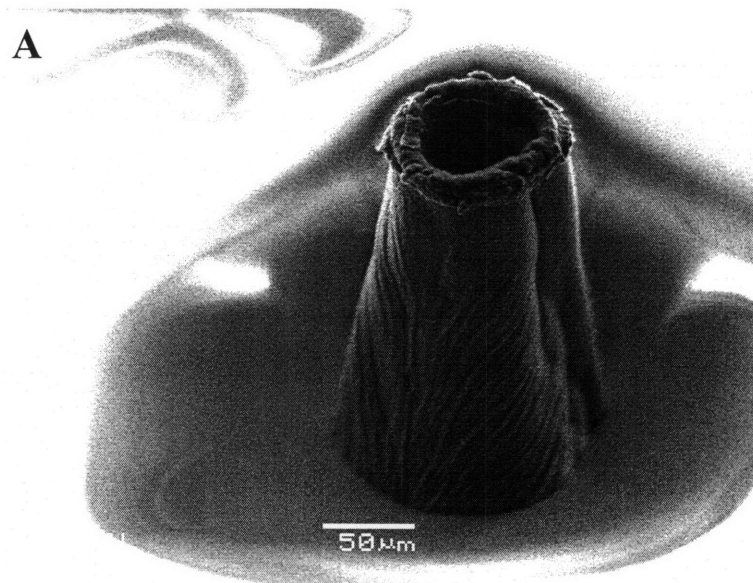
Finally, their high cost (~\$200-600) limits their availability to basic research laboratories and effectively precludes their use in high-throughput screening settings, where, in contrast, cheap, disposable units are required.

Various proof-of concept demonstrations have been reported in the literature using chemical and physical cues to construct networks of controlled connectivity(Claverol-Tinture et al., 2005, Beom Jun et al., 2005, Jun et al., 2007, Leng et al., 2004, James et

al., 2004, James et al., 2000{Tooker, 2004 #56, Tooker et al., 2005); however, to our knowledge activity-dependent synaptic plasticity, essential to recapitulate the in vivo situation, has not been successfully employed to create large networks of controlled connectivity, although in-vitro neuronal networks have been for almost two decades a field of very active research.(Rolston et al., 2007, Wagenaar et al., 2006a, Wagenaar et al., 2006c, Wagenaar et al., 2006b, Breckenridge et al., 1995, Jimbo et al., 1993, Claverol-Tinture et al., 2007)

1.2 Our approach

We aimed to overcome some of these limitations by employing an array of columnar electrodes made from a conducting polymer (polypyrrole). This geometry, combined with the surface roughness of polypyrrole (see Fig.1) and adhesion molecules (such as oligopeptides from the laminin sequence) that can be easily incorporated in the polymer should allow much better contact between cells and electrodes. At the same time, their height would allow growing a feeder monolayer of glia before seeding the neurons, while ensuring direct contact between the neurons and the electrodes



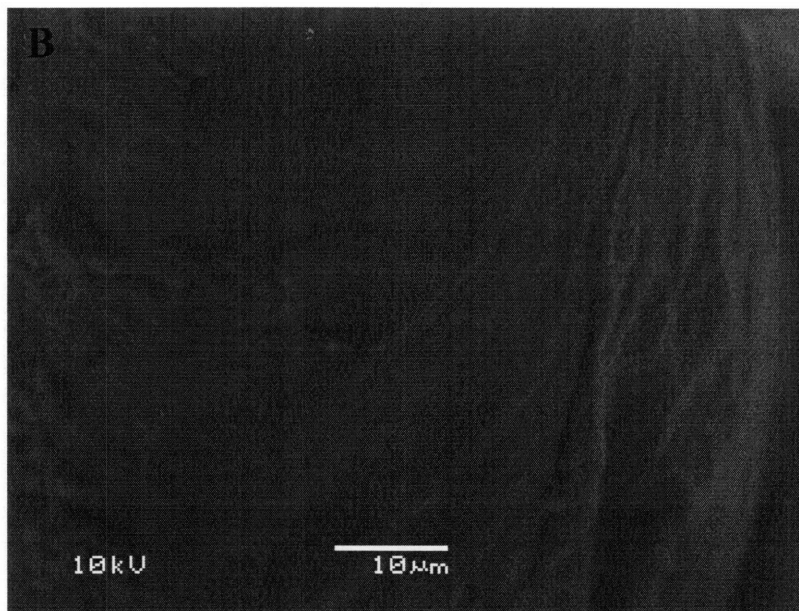


Figure 1. A. SEM image of a single 500µm-tall NaDBS/PPy pillar, embedded in a 250µm-thick implant-grade PDMS sheet. B. SEM image of the lateral surface of the same.

The electrodes are to be used only for stimulating the neurons, while the response can be recorded by employing calcium-sensitive dyes and wide-field optics. This will permit simultaneous monitoring of the whole network activity in the culture, free from stimulation-induced artifacts.

Finally, polypyrrole electrodes, embedded in an elastomeric insulating substrate, can be made for a fraction of the price of current electrodes, to create a disposable chip integrated in a fixed setup containing the underlying electronics and imaging systems.

In order to drive the system, we developed a simple software interface that, in conjunction with 64 channels output, allows on-the-fly individual, simultaneous control of the waveform output from each electrode.

1.3 High-throughput cell-based drug screening

Arguably the single greatest advantage over existing technology will be the possibility to carry out high throughput screens on small compounds libraries for identification of neuropharmacologically relevant molecules.

High-throughput screens have become a mainstay in drug research (Orry et al., 2006, Wu and Doberstein, 2006, Broach and Thorner, 1996), often in conjunction with target-based rational drug design, to optimize the potential relevance of the chemical space searched, and thanks to its high level of automation, it allows rapid screening of millions of compounds to identify promising leads.

Until recently, however, most screens were limited to measuring interactions of the various compounds against an isolated ligand, outside of the complex cellular environment, leading to relatively large numbers of false positive and false negatives. More physiological and effective cell-based screens are starting to emerge (Castel et al., 2006, Balimane and Chong, 2005), but until now it has not been possible to apply such techniques to the electrophysiological, long term study of neurons or cardiomyocytes, arguably the two most important cell types for clinical applications.

1.4 Neuronal plasticity

From early development to adult life, plasticity is one of the essential elements of neural networks wiring. While during development extensive rewiring tends to occur, in adulthood in higher mammals most plasticity occurs by regulation of synaptic strength.

According to its mechanistic basis, as well as according to the timescale on which it operates synaptic plasticity is commonly subdivided into short-term plasticity (operating on the timescale of tens-hundreds of msec), synaptic modulation (seconds), long-term potentiation (LTP) and long-term depression (LTD, with a timescale of minutes to hours), spike-timing dependent plasticity (minutes to hours) and homeostatic plasticity (days)

1.5 Spike timing dependent neuronal plasticity (STDP)

Spike Timing Dependent Plasticity (STDP) is a form of synaptic plasticity believed to strengthen synapses that are activated within 20 to 40 ms before a postsynaptic spike, and

to weaken those that are activated within a similar time window after the spike (Dan and Poo, 2004, Dan and Poo, 2006, Constantine-Paton, 2006).

At many synapses, the induction of spike timing-dependent LTP/LTD requires activation of the NMDA subtype of glutamate receptors (NMDARs) (Markram et al., 1997, Bi and Poo, 1998) In some cases, LTD induction was also shown to require the activation of L-type Ca^{2+} channels (Bi and Poo, 1998) and Ca^{2+} release from internal stores (Nishiyama et al., 2000).

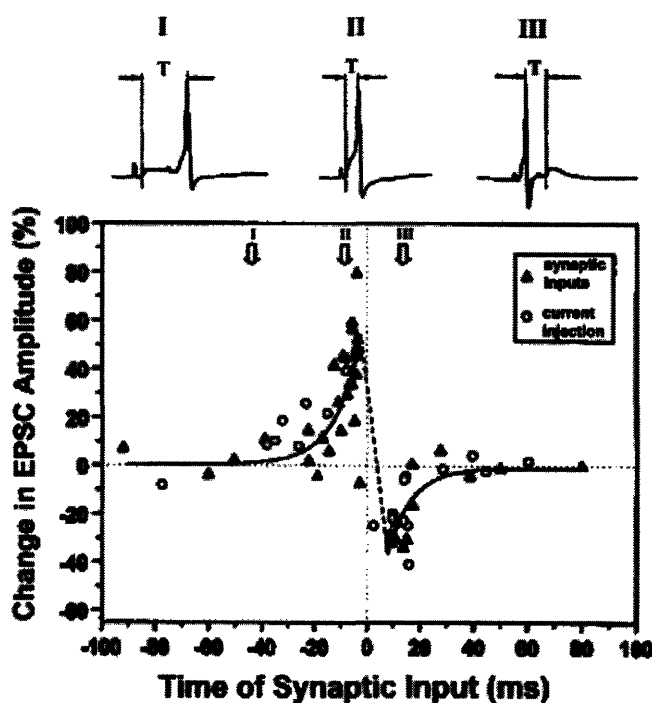


Figure 2: The Critical Window for Spike Timing-Dependent Plasticity of Developing Retinotectal Synapses(Zhang et al., 1998) ©Nature Publishing Group. Reprinted with

The first explanation for the temporally asymmetric STDP that was put forward is that the relative timing of glutamate binding to NMDARs and the spiking of the postsynaptic dendrite determines the Ca^{2+} level required for either LTP or LTD (Barth and Malenka, 2001, Zakharenko et al., 2001, Bi and Poo, 1998).

However, this model doesn't account for all the observations available; in particular, topics of active investigation are the varying width of time windows for depression and potentiation for different neuronal subtypes and even for the same cell population subject to external modulation(Zhang and Linden, 2003, Sjostrom et al., 2003), the exact dynamics and extent of post vs. presynaptic modifications(Sjostrom et al., 2003), as well as the role of STDP in neuronal development, memory and learning (Buchs and Senn, 2002, Song and Abbott, 2001, Boettiger and Doupe, 2001, Bi and Poo, 2001, Abbott and Nelson, 2000, Song et al., 2000)

Our work will entail designing and building a proof of concept device, and use it to grow networks of cultured dissociated neurons to investigate STDP at two levels: at the network level and at the individual synapse level. On one hand we are interested in exploring the use of time- and space- specific stimulation to grow networks of controlled connectivity, possibly in conjunction with known chemical guidance cues. On the other hand, we aim to further elucidate the fundamental biochemical mechanism underlying spike-timing dependent plasticity using both genetic knockout models and inhibitory compounds to selectively block specific cellular pathways.

1.6 Conductive polymers

Electrically conducting polymers are a relatively recently developed class of materials(Hush, 2003, BA Bolto, 1963, R McNeill, 1963), that has already found considerable application as, among other things, actuators, sensing elements, and for the fabrication of electronic components

Virtually all common conducting polymers (e.g. poly(acetylene)s, poly(pyrrole)s, poly(thiophene)s, poly(aniline)s, poly(fluorene)s, poly(3-alkylthiophene)s) have conjugated backbones with a high degree of π -orbital overlap (Wong et al., 1994, Kanatzidis, 1990, Iseki et al., 1991)). Through a process known as doping, the neutral polymer chain can be oxidized or reduced to become either positively or negatively charged respectively, with polarons and bipolarons as the charge carriers for electrical

conduction. The conductive form of the polymer contains counterions which serve to maintain charge neutrality but does not alter the oxidation level of the polymer.

The dopant ion is essential in determining the structural properties and the electroactive behavior of the polymer. As the polymer is switched between the conductive and insulating states, the dopant ions diffuse in and out of the polymer(Iseki et al., 1991).

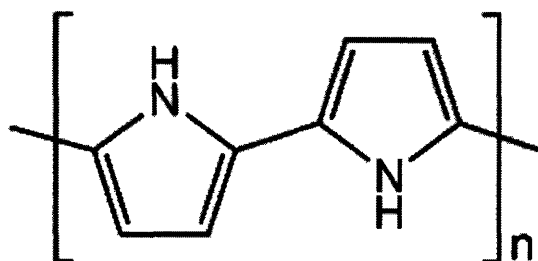


Figure 3: Chemical structure of polypyrrole

1.7 Polypyrrole in biotechnology

Polypyrrole has found use in biotechnology applications, thanks to its established biocompatibility(George et al., 2005, Wang et al., 2004a), as well as ability to incorporate a variety of biologically-relevant moieties and good conducting properties.

Both its electroactive properties and the possibility to incorporate growth factors and adhesion molecules have been used to help control cell morphology and behavior in vitro(Song et al., 2006, Stauffer and Cui, 2006, Schmidt et al., 1997, Wong et al., 1994, Kotwal and Schmidt, 2001, Gomez and Schmidt, 2007)

A recent, promising use has been as a coating for neural probes, with the aim to to improve neuronal adhesion and reduce glial scarring(Cui et al., 2003). For clinical tissue engineering application, PPy composites have received a certain degree of attention as potentially useful materials for nerve regeneration scaffolds, especially when combined with biodegradable polymers such as PLLA (Keohan et al., 2007, Kim et al., 2004, Zhang et al., 2007),

Finally, controlled drug release applications have also started to be explored (Wadhwa et al., 2006).

2. ELECTRODE STIMULATOR

The use of activity-dependent plasticity in patterning ensembles of neuronal populations requires precise control over the stimulation of each subpopulation with high temporal and spatial resolution, and the ability to simultaneously address different populations.

Unlike the commercially available microelectrode array systems, which have been designed with an emphasis on electrical recording and stimulation being limited to one, or at most, a few electrodes, we designed our system to be a highly parallel stimulation system, relying on optical methods to record neural activity. This posed engineering problems fundamentally different from those addressed by previously described devices. Furthermore, while the electronics themselves could be as complex as needed, we wanted the interface to be very intuitive.

2.1 All-channel stimulator

Our initial approach was based on work by Wagenaar and Potter^(Wagenaar and Potter, 2002) on a stimulator for microelectrode arrays, controlled by a PC running a real-time operating system (in our case, RTLinux).

Of relatively simple construction, relying on a single 8-bit Digital-to-Analog Converter (DAC) (TLC7628, Texas Instruments), the design allows selection of any electrode in a standard 64 electrodes array, and rapid ($\sim 10 \mu\text{s}$) switching between different ones.

The stimulator consists of one main board containing a DAC and interface logic, as well as four modules each of which contains isolation switches to gate signals to one of 16 electrodes. It is controlled from a PC's parallel port, which provides four 'control' pins and eight 'data' pins. The control pins are used to route signals from the data pins to either of two DAC channels—one for the stimulus proper, one for an auxiliary analog output. A kernel module for RTLinux to control output voltages and switching with high

temporal accuracy was kindly provided by Dr. Wagenaar. A higher-order programming language, Perl, (www.perl.org) was used to more easily program stimulus waveforms.

Despite its relative simplicity and power, the system still presented serious shortcomings. Aside from being somewhat unreliable and crash-prone, it didn't allow truly simultaneous stimulation of all electrodes, wasn't easily scalable and, importantly, wasn't very user-friendly. Finally, data acquisition and stimulation couldn't easily be integrated.

2.2 64-channel, integrated stimulator

To address these problems, we combined a very simple graphical interface (Figure 4)

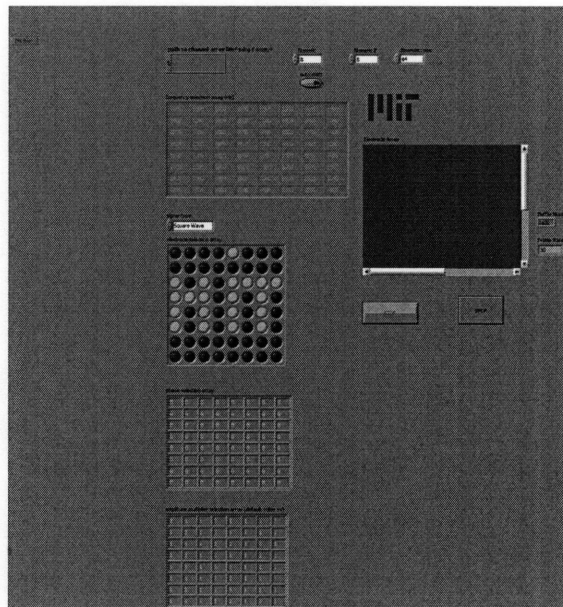


Figure 4. Graphical user interface to electrode stimulator.

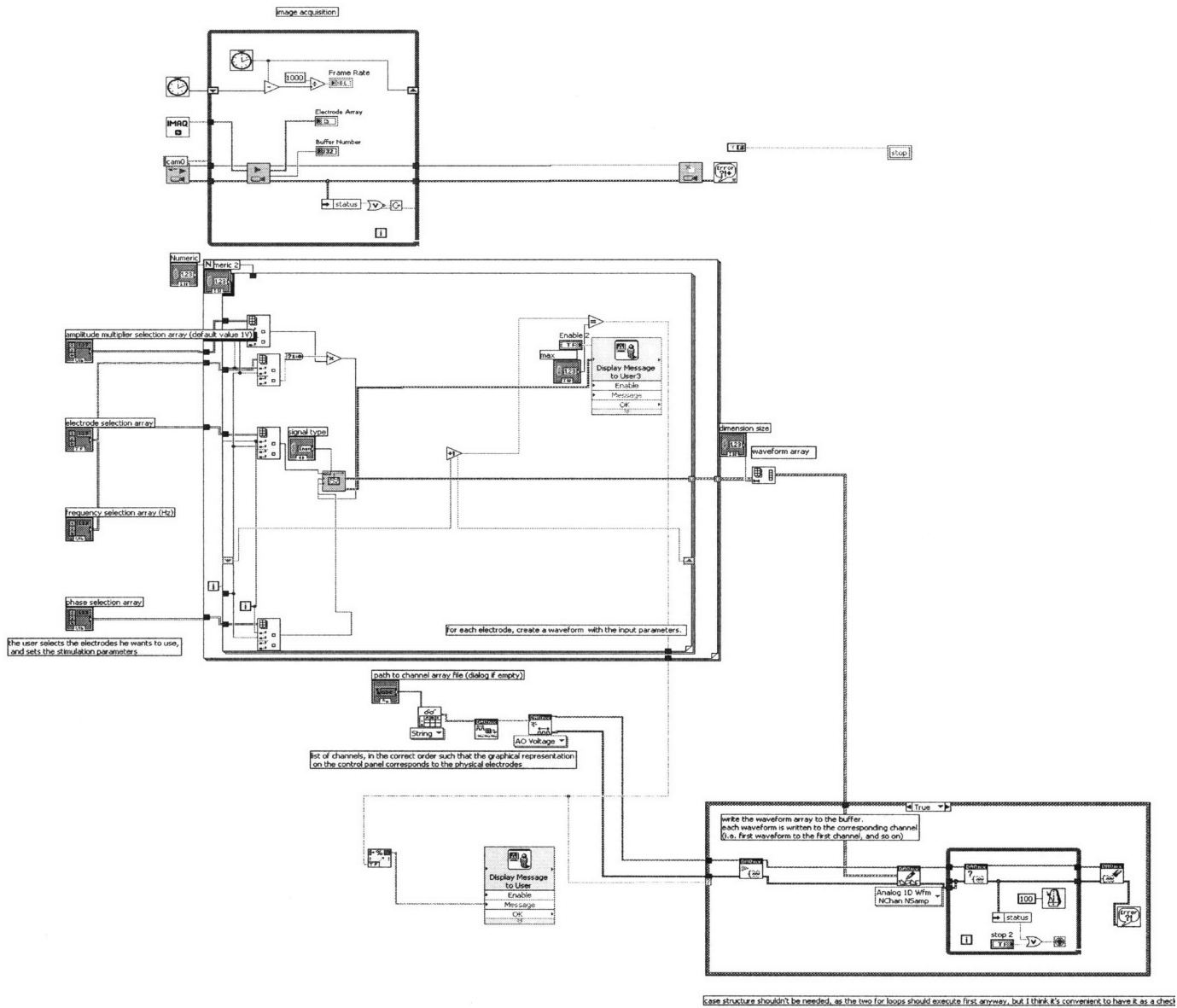


Figure 5. Schematic of stimulation and image-capture software.

with two high-end multifunction data-acquisition cards (DAQ) (NI PCI-6723, with 32 analog output channels, connected so as to functionally act as one, with 64 channel device) for allowing independent control of up to 64 channels. This allows the user to rapidly specify an arbitrary pattern of stimulation for each of the electrodes in the array, and even modify it in real time, while simultaneously imaging the culture. Note that, for high-throughput applications, the rapid-switching electronics from the first implementation could be combined with the second implementation's 64-channel

capabilities, thus allowing control of several arrays at once. If the full 64-channels stimulation capability is not required for each array, the later could be separated into smaller subchambers (enclosing, e.g., 4x4 electrodes), driven by specific stimulus patterns.

The whole system was implemented in the LabView 8.3 (<http://www.ni.com/labview/>) environment, combining simplicity, ease of modification in response to changed research requirements, and power. An advantage of this choice is the availability of advanced data analysis tools that can be integrated into the imaging and stimulation system, potentially allows for the development of “smart” stimulation protocols that adjust to the electrophysiological behavior in real time.

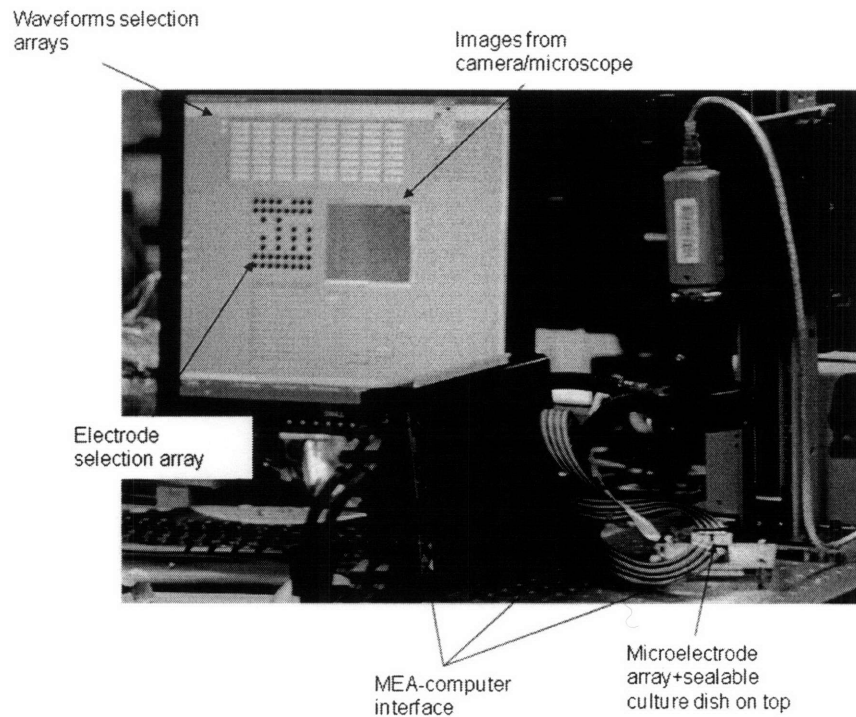


Figure 6. The complete stimulator, interface, and (testing) image acquisition system.

2.3 Interface and testing

From the DAQ, the output wires were connected to a custom-made PCB board that interfaced with the EA via spring-loaded connectors. To test the ability of the reversible PDMS-glass bond to ensure stable electrical contact, the electrode array was either adhered to a uniformly conducting Indium Tin Oxide (ITO) or Glassy Carbon (GC) electrode, or carefully aligned and positioned on top of the MEA, while electrical connection was tested by passing current-regular probe on contact pad (millimeter-scale), while the PPy electrodes were contacted by a needle-like electrode mounted on a micromanipulator. An alternative approach would have been to conduct the characterization in a bath, obviating the need of painstaking aiming of the probe at the micropillar, but problems with underlying insulation of MEA made it hard to reliably stimulate just a single pillar. The results, very preliminary, indicate a pillar resistance, taking into account contact resistances, on the order of $1\text{k}\Omega$.

2.4 Electrode substrate

As a first step for proof-of-concept validation we used old commercial MEAs (MCS GmbH). In general, the permanent electrode array onto which the PMEAs will be laid could be easily fabricated with standard photolithographic techniques on, e.g. ITO or even polymeric substrates such as PDMS.

An interesting alternative for high-throughput screens applications, in combination with top-only illumination and imaging, could be to use standard PCB boards. Since PDMS doesn't bond to the bare board, we have found spraying the surface (after masking the contact pads,) with a silicone-based electronics sealant to be very useful for allowing a good seal.

Transparency masks for single 8x8 electrode arrays, as well as 4x4 and 8x8x96 electrode arrays were designed and printed, to enable fabrication at the MIT Microtechnology

Laboratory: an important consideration given the extremely high cost (\$200-600) of commercial MEAs.

In order to start working on plasticity-driven neuronal network patterning, we fabricated cell-culture chambers on top of old commercial MEAs, and cultured mouse embryonic hippocampal neurons (see Appendix 1 for the cell dissociation and culture protocol used)

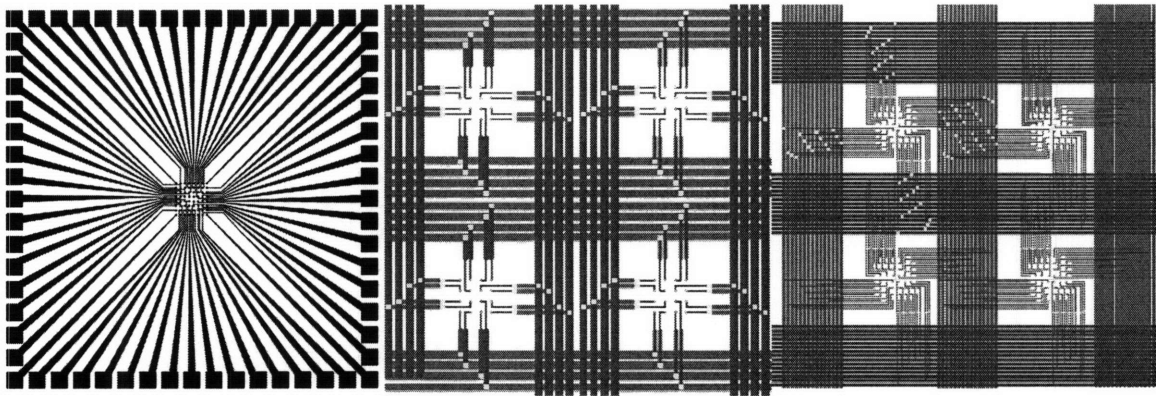


Figure 8: A. mask for a single 64-electrode array, B.,C. 4x4 wells patch of 96-well 16 and 64 electrodes/well array, respectively.

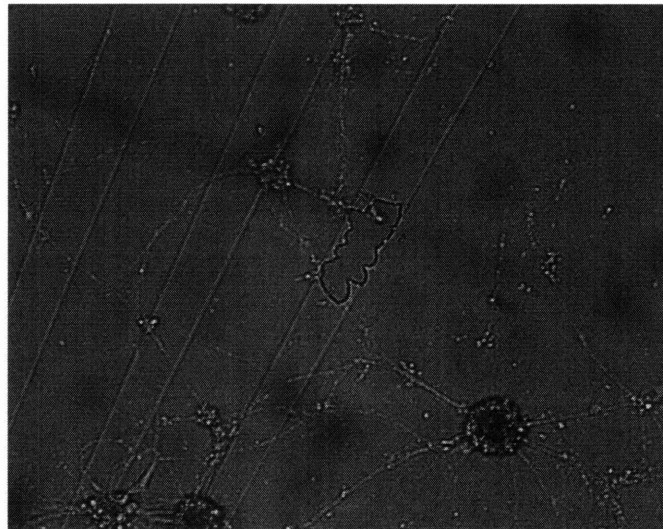


Figure 9: 4-week old neuronal culture on a commercial MEA, coated with fibronectin. Two of the problems that plagued them are readily apparent: the poor hydrophilicity of the substrate led to cell clumping, detachment and death, while the insulation tended to “flake off”

Initially we ran into considerable surface hydrophobicity issues, which were only resolved after we gained access to an asher, and didn't have time to test them. The poor condition of the insulating layer, which had flaked off the surface in several points would have seriously hindered experiments anyway. Hence the need to fabricate our own microelectrode arrays, a relatively straightforward process.

3. PMEAs

3.1 Fundamental constraints: biocompatibility and amenability to mass fabrication

The fundamental design constraints for the all-organic microelectrode array were suitability for long-term cell culture, as well as ease and low cost of fabrication, to enable its use for both fundamental neuroscience research and high-throughput industrial applications.

While each constraint could be met relatively easily on its own, satisfying them simultaneously required the development of novel fabrication techniques and judicious material choice and standards, especially in light of the particular sensitivity of primary neuronal cultures. Unlike more commonly used immortalized cell lines, primary neurons are exquisitely sensitive to even the most minute amount of contaminants or deviation from optimal culture conditions.

Among the existing conductive polymer, PPy appeared as particularly promising for our application (see Section 1.6); as inert, insulating substrate, the choice fell on implant-grade polydimethylsiloxane (PDMS), a silicon-based organic elastomer that has already found extremely widespread use in biotechnology and medicine.

3.2 Polypyrrole micropillar fabrication techniques

3.2.1 Free growth on EDM'd array

A way of making arrays of free standing PPy spikes, embedded within an insulating (e.g. PDMS) layer, building upon several aspects of the work of Fofonoff et al. (Fofonoff et al., 2004) would be to fabricate arrays of glassy carbon pillars (see Figure 10), which would then be used as controlled growth sites of the PPy pillars (see Figure 11).

To fabricate these master arrays, electric discharge machining (EDM) would be employed. EDM is a machining technique in which metal is removed by generating high frequency sparks through a small gap filled with a dielectric fluid between an electrode and the material to be removed. It has been successfully used in the fabrication of electrode arrays for neural implantation, and can achieve feature size on the order of $\sim 100\mu\text{m}$. Among its distinct advantages, are the ability to quickly machine a wide range of materials, as well as its relative ease of use, and the ability to handle complex geometries.

In our envisioned process, only the very tip would be kept in contact with the electrodeposition bath at any given moment, as the array is progressively raised, so as to obtain an almost entirely axial growth of the PPy structures.

The construct would then be inserted into an insulating mask, a sealant coating would be spun on top to ensure tight adhesion of the two, then the pillars would be cut flush with the bottom of the mask by EDM.

This approach would allow the fabrication of very large sets of arrays in parallel, and fabrication of the masters would be relatively simple and inexpensive.

However, the proposed technique also suffers from a number of distinct disadvantages. For example, it would require a very uniform rate growth of PPy across pillars, as well as excellent control of timing to prevent lateral growth, and some degree of variability across pillars would probably be inevitable. Moreover, while the fabrication the PPy pillars themselves is at least conceptually very simple, a number of additional steps would be required to obtain the complete device, including fabrication of separate mask, alignment, sealing, and trimming the pillars exactly flush with the substrate.

3.2.2 Free growth on planar MEAs

As a first step to study the effect of 3D geometry on neuronal cell cultures, we investigated the possibility of growing PPy directly onto planar MEAs, possibly in the presence of a surfactant to enhance growth anisotropy (Carswell et al., 2003). Although one such array was in fact produced, we chose to focus on developing more scalable fabrication techniques, as this approach would only introduce further complication and cost to the already expensive process of MEA fabrication.

3.2.3 Interstitial deposition, PPy-PDMS nanocomposites

A third approach that was explored was to embed the PPy within a more easily moldable or shapeable polymer network, in a fashion similar to what had been done to incorporate conducting polymer into biodegradable materials (Shi et al., 2004, Wang et al., 2004b, Wang et al., 2003, Zhang et al., 2007). The general approach would be to either add PPy nanoparticles to a polymer which will then be micromolded, or micromold a polymeric spike array, then put it in a suitable solvent and deposit PPy within the network of spaces of the primary polymer.

We made structures out of PDMS, swelled them in THF, then used electroless deposition technique to embed PPy within it. Although some deposition within the host polymer was observed both in flat 250 μ m sheets and molded microspike arrays, we obtained only very poor conduction ($\sim 40,000 \Omega \text{ m}$), which was moreover mostly due to a surface layer of more uniform PPy. There were also concerns with the possibility of residual THF traces poisoning the cell cultures. Overall, while this technique did show some promise, it was finally deemed unsuitable for our specific application, especially in light of the development of better mask-based fabrication protocols.

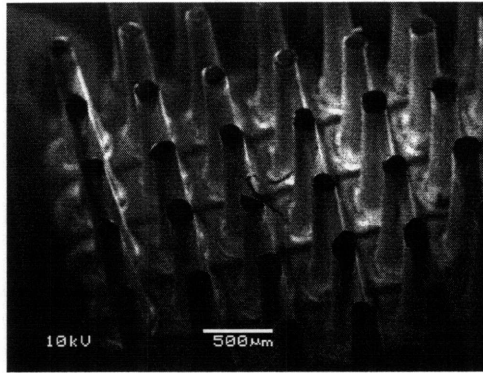


Figure 12: micromolded array of PDMS pillars

3.2.4 Electrodeposition through a mask

3.2.4.1 Mask fabrication methods

The method ultimately selected for the fabrication of conducting polymer spikes was to use a mask, to be either removed or used as the insulating substrate, to constraint the polymer growth during electrodeposition.

Mask-based microfabrication techniques could be employed in two broad fashions. One approach would be making the mask integrated with MEA, by making a planar MEA with standard photolithographic techniques, then adding an extra photoresist layer, patterning it and using it as a mask for PPy electrodeposition. While viable in a research setting, this would offer no improvement in terms of cost compared to currently available devices.

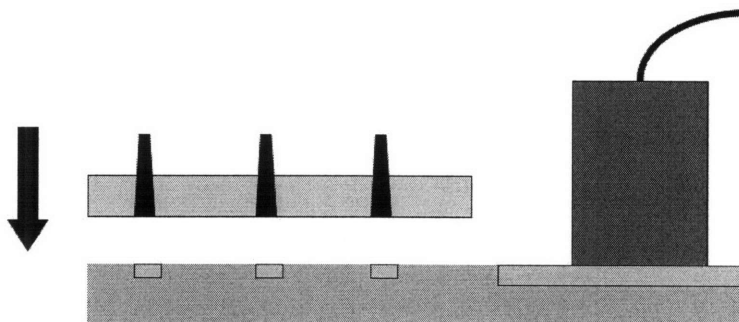


Figure 13: interfacing the disposable PMEA with the fixed stimulation setup

The other approach, which we chose to follow, is to make inexpensive, disposable, arrays of conducting polymer embedded in the insulating substrate, which, for use, would be reversibly sealed to a fixed electronic interface (see Fig. 13)

Although using nanopatterned templates for growing nanotubes and nanowires has been previously described, it had never been used for fabricating distinct 10 to 750 μm structures. The conceptual simplicity of this approach made it highly appealing, but a number of technical difficulties had to be addressed. First and foremost, a method had to be developed to fabricate micron-sized templates inexpensively from biocompatible materials. Secondly, the nonlinearities and problems of unusual PPy electrodeposition conditions, very different from the standard micron-thick uniform films had to be dealt with. Other important issues were how to ensure extremely tight, but reversible, seal between the mask and the electrode used for PPy electrodeposition and, finally, how to integrate the construct into the final device.

Molding

Since photolithographically-defined master arrays up to $\sim 300 \mu\text{m}$ tall, or EDM's arrays up to 1.2 mm tall could be fabricated, one approach to mask production that we investigated was to spin coat them with an insulating material (SU8, PDMS, PMMA, etc.), which would then be cured and detached.

Problems encountered with this approach were removing the mask from the master, especially at smaller feature sizes, difficulty of handling the very thin masks, and difficulty to scale up in volume fabrication.

Punching

An alternative that we actively pursued was to start with flat, inexpensive PDMS sheets, and punch the desired pattern with a master, either an EDM'd array, chemically sharpened (kindly provided by Tim Fofonoff, M.S.), or glass or quartz pulled

micropipettes, pulled with a Sutter Instruments 2000 laser-based pipette puller, of tip diameter ranging from $\sim 10\ \mu\text{m}$ to $\sim 100\ \mu\text{m}$. In order to provide repeatable results, the pulled micropipettes were mounted on a 3-axis micromanipulator, that allowed arbitrary patterns to be quickly produced. After alignment, the punch was brought down onto the substrate, which rested on a thick piece of PDMS, so that complete penetration of the mask material could be achieved with limited damage to the punch.

Although this technique proved feasible for investigating the use of a mask for growing the desired PPy micropillars, and could be used to create features down to a few tens of micrometers, it also suffered from distinct disadvantages.

The EDM'd arrays were complex to fabricate and got damaged after a few uses, and would have had to be regularly replaced. Furthermore, micropillar size was effectively limited to a minimum of approximately $100\ \mu\text{m}$. The micropipettes on the other hand were too fragile for continuous use (although switching to quartz did ameliorate this issue) and not suitable for fabricating anything other than very small arrays on a limited basis.

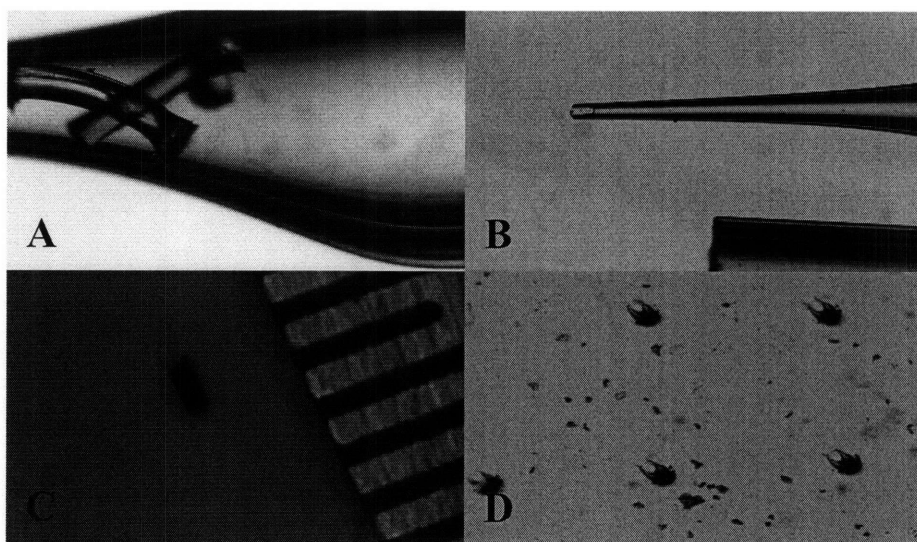


Figure 14. A. PDMS cylinders punched out by the micropipette. The high aspect ratio achievable is evident B. Micrograph of a $\sim 75\ \mu\text{m}$ glass micropipette-notice how the tip broke after only a few uses. C. Single PPy microelectrode, broken off from the glassy carbon electrode surface for imaging. divisions are $500\ \mu\text{m}$. D Micrograph of the upper left portion of an octagonal pattern of 20 electrodes. The film is under slight shear strain

The use of arrays of micropipettes was limited by their shaft diameter (which limited how closely spaced together the micropillars could be), and, most importantly, by their fragility, which would have made them much too unreliable.

Laser patterning

The technique we ultimately selected for mask fabrication, because it offers at the same time sufficient resolution, flexibility and high throughput is laser micromachining

An unusual property of laser micromachining is that when drilling through holes, the entrance diameter is larger than the bottom hole diameter; the typical half angle side-wall taper is 3 to 7 degrees, depending on material, depth of focus, beam profile and fluence.

While this is normally a problem in micromachining applications, it was in fact desirable for our application. Conical pillars help ensure a good electrical contact between the PMEA and the fixed electronics, and make it easier to remove the mask surface layer after deposition is complete.

A variety of lasers can be employed, each with specific advantages and drawbacks, and range of applications. The most common ones are carbon Dioxide (CO₂), Diode-pumped Solid State Lasers (DPSS), Excimer lasers and Femtosecond lasers.

CO₂ lasers are gas powered lasers that operate in the infrared spectrum (10.6 micrometers) with average powers in the kilowatts with high repetition rates; practically, the smallest spot size achievable is 50 to 75 microns diameter, with feature resolution normally larger than 200 μm.

DPSS (such as Nd:YAG and Nd:YLF) are solid-state lasers that are pumped by a series of diode bars. While their fundamental wavelength is 1.06 micrometers, non-linear crystals can be used to double (532 nm), triple (355 nm) and quadruple (266 nm) the laser wavelength, albeit at the cost of lower average power.

Excimer lasers are gas powered lasers, often filled with a mix of fluorine and argon. The excimer laser achieves the highest average power (up to 100 W) in the ultraviolet spectrum, with laser wavelengths ranging from 157 nm, 193 nm, 248 nm, 308 nm and 351 nm, and can reach practical resolution in the 1 μm range.

By operating in the ultra-violet region, the excimer laser ablates the material by breaking the molecular bonds within it. The ablated material is ejected upward and away from the material surface at supersonic speed, while thermal effects are minimized, allowing much smoother surface finishes and preventing substrate degradation

The excimer laser has a typical pulse duration of 20 nsec, at a repetition rate up to 200Hz with an etch rate of approximately 100 to 500 nanometers per pulse, so that substantial thicknesses can be ablated in reasonable times.

Femtosecond or ultrafast lasers are solid state lasers that produce a temporal pulse in the femtosecond regime (10^{-15} s). Although they are very promising, they are at the present time mostly confined to research applications

DPSS, femtosecond and CO_2 lasers utilize a direct write approach, and excimer lasers can also be used in this mode, in addition to mask projection techniques. The laser beam is focused to a small spot size, and the beam traces out the pattern to be cut. Direct write lasers are especially suitable for prototyping, as a pattern drawn in a CAD program can immediately be transferred to the substrate, without need of making a mask first.

In fact, most of the development work on the PMEAs was carried out with a CO_2 laser in the direct-write mode. While the resolution of our system was coarser than we desired, by taking advantage of the tapered geometry of laser-drilled holes, we could easily achieve micropillars with tip sizes of only 75 to 100 μm , comparable to commercially available microfabricated MEAs. We used PDMS masks 500 μm thick to ensure ease of handling; however, this forced us (given the power of our CO_2 laser) to use multiple shots for each mask well. Going to thinner masks (e.g. a bilayer made from a 125 μm implant grade

sheet and 30 to 40 μ m spin-coated PDMS) or employing more powerful lasers could allow using single pulses, and obtaining smaller features.

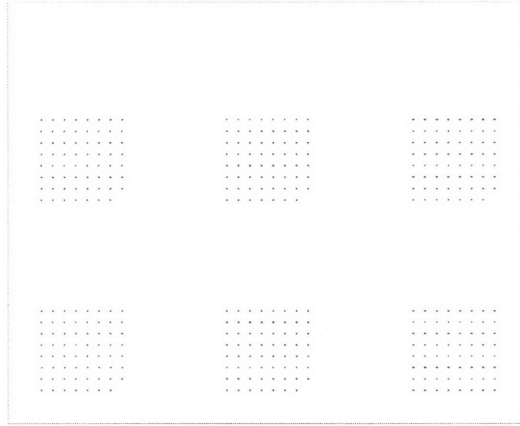


Figure 15. CorelDraw drawing (magnified) of a typical 6 x 63 electrodesmask, used in conjunction with 25mmx25mm glassy carbon electrodes. The pattern is directly "printed" into the PDMS bilayer.

However, much thinner masks would be would be considerably more difficult to manipulate, and acquiring a completely new laser system would be prohibitively expensive at this stage of development.

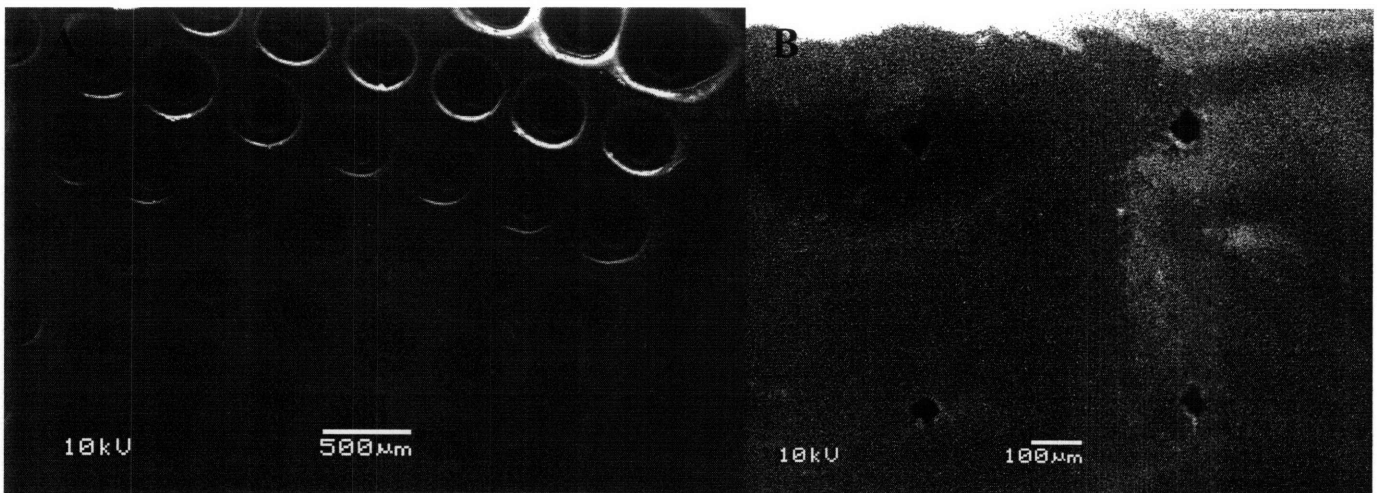


Figure 56. Scanning electron micrographs of laser-patterned masks, showing the bottom (wider) (A) and top surface (B).

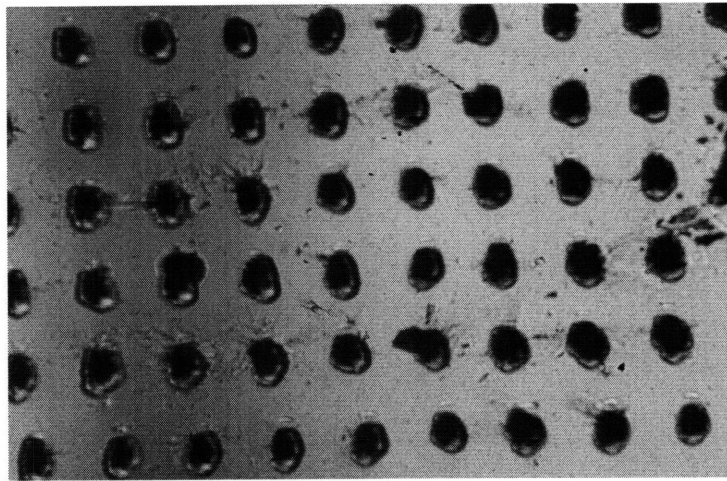


Figure 17; an early deposition on ITO of PPy/NaDBS using a monolithic 250 μm -thick mask, before etching the mask. The pillars are 450 μm apart.

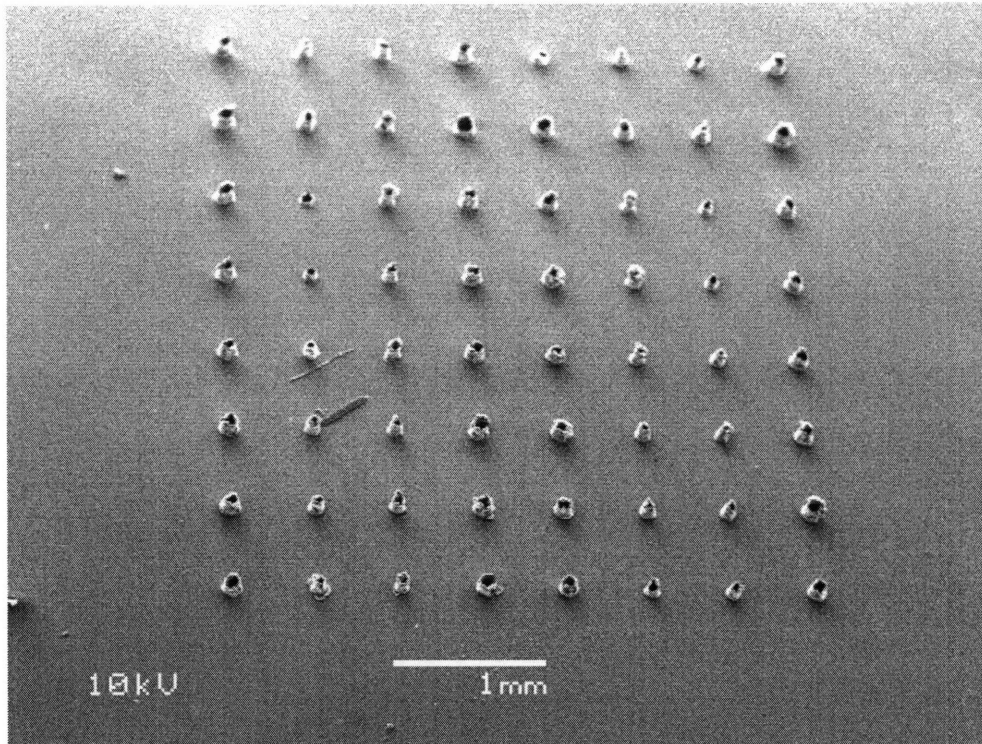


Figure 18. SEM of the first micropillar array grown through a 250+60 μm thick mask.

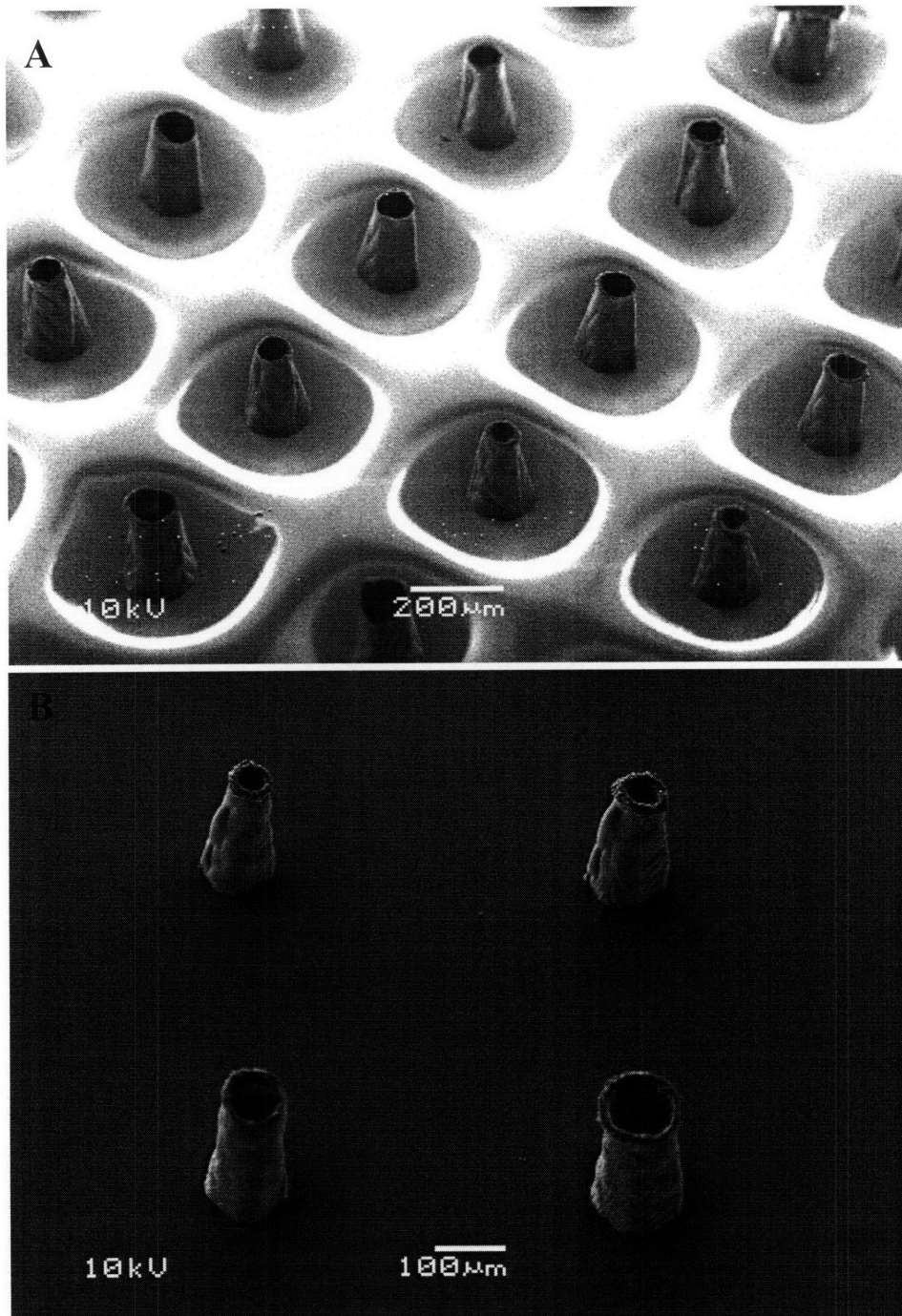


Figure 19; A. SEM of a portion of a typical 63-electrode PPy micropillar array grown through a 250+250 μm -thick PDMS mask. B. Enlarged image of a portion of the same array, after gold-coating the sample to get rid of the “show-through” effect present with the uncoated PDMS. The variability in size of the very tip of the micropillars was due to some of them growing to the top of the PDMS mask and starting to flare out before the end of the deposition process, and was eliminated with better control of the deposition process.

In order to improve onto electrode size, to bring it on par with the very best commercially available electrodes (10 μm), we started exploring the sue of excimer lasers. In addition to direct write mode, excimer lasers are also suitable for a variety of mask-based techniques, such as mask projection laser drilling, multiple beam system, contact mask, coordinated opposing motion (www.resonetics.com)

The excimer laser illuminates a mask (which is not in contact with the part) that contains a pattern: this pattern is imaged by downstream optics to produce an identical, demagnified pattern. Unlike with more conventional laser micromachining systems, features as small as 1 μm can be produced.

Usually, the mask is fabricated inexpensively with a pattern that is typically 150 micrometers or greater. Since the mask projection technique optically reduces or " the mask pattern by 5 to 30 times, low cost methods can be used to fabricate the mask

Mask projection techniques offer distinct advantages over direct write approaches, both in terms of pattern quality and in terms of throughput, as even complex shapes can be flawlessly produced, with perfectly shaped edges, and several patterns can be machined in parallel. Especially if combined with holographic optics, which can produce a dense array of laser beams (potentially thousands of beamlets) at one time, this makes excimer lasers eminently suitable for high-throughput manufacturing of the pMEA masks.

Early trials has shown that it is indeed possible to pattern PDMS bilayers and even PDMS-glass-PDMS trilayers with features approaching 10 μm , and grow PPy through it, confirming this a potentially very powerful method to pursue.

3.2.4.2 PPy electrodeposition

Most commonly polypyrrole dopant ions and deposition conditions are optimized in light of the polymer's use as an actuator or sensing material; in particular, our laboratory has developed a variety of protocols involving the potentiostatic deposition of doped polypyrrole in a propylene carbonate bath. In contrast, for devices meant for long-term cell culture, biocompatibility becomes the overwhelming concern, so that both dopants and solvent need to be as innocuous as possible, without excessively compromising conductivity.

We eventually settled for a high-pyrrole-monomer-concentration (0.1 to 0.2 M), aqueous galvanostatic (10 to 30 A/m²) deposition of PPy doped with either sodium dodecylbenzenesulfonate (NaDBS, Sigma-Aldrich), polystyrene sulfonate (PSS, Sigma-Aldrich), or hyaluronic acid (HA, Sigma-Aldrich), carried out at 25° C.

Varying the deposition temperature and dopant of choice led to some variation in surface morphology, with films deposited at lower temperatures (4° C) showing a more irregular surface, and greater variation in thickness, while conductivity was effectively the same across all conditions, at approximately 2 to 2.5 kΩ m.

From preliminary experiments all chemistries seem to support cell growth, in agreement with the literature , and showed good adhesion to ITO. While both PPy/NaDBS and PPy/HA grew best on glassy carbon electrodes, forming uniform, PPy/NaDBS tended to adhere very strongly to glassy carbon, PPy/HA could be more easily released, making it the composition of choice for most experiments. Although HA tends to be cell-repellent, laminin and PLL bind strongly to it, so that after incubation PPy/HA/PLL-laminin shows good cell-adhesive properties

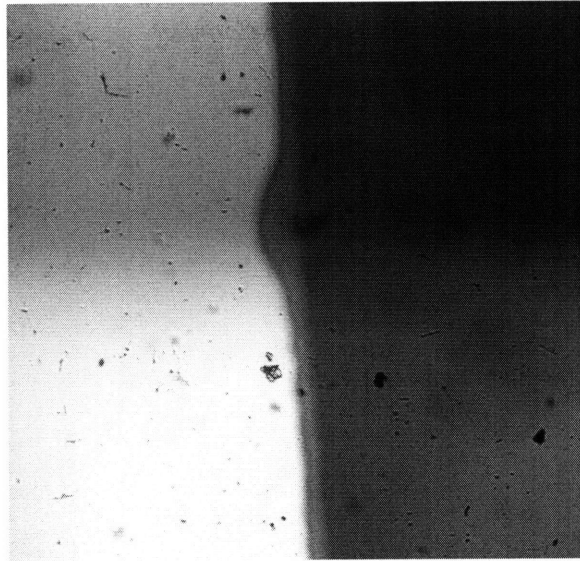


Figure 60; various surface chemistries tested in culture. From the top left, clockwise: PPy/HA, PPy/HA grown on top of a PPy/NaDBS substrate, PPy/NaDBS, bare ITO-coated glass.

By controlling pyrrole concentration, current and deposition time we could reliably control the topology of the deposited microstructures, forming either microtubes (with walls of predictable thickness) or solid microwires, up to 750 μm tall.

The ability to controllably grow PPy tubular structures at the microscale, with diameters ranging from 10 to 250 μm and height greater than 500 μm shows great promise, in addition to the fabrication of cellculture arrays, to application in MEMS actuation and sensing. The same technique also allows for the deposition of multilayered structures.

An interesting possibility raised by the use of excimer lasers for the fabrication of the masks, allowing the creation of structures on the 10 μm scale, is the use of the micropillars themselves (mechanical properties, spacing, etc.) to influence cell behavior. Microscale patterns have also been shown to greatly affect the cellular microenvironment ,see for example (Flemming et al., 1999) for a review. An interesting and relevant application of microtextured substrates uses 10 μm micropillars to prevent overproliferation of contaminating fibroblasts in cardiac myocyte cultures without the use of cytostatin.(Boateng et al., 2003)

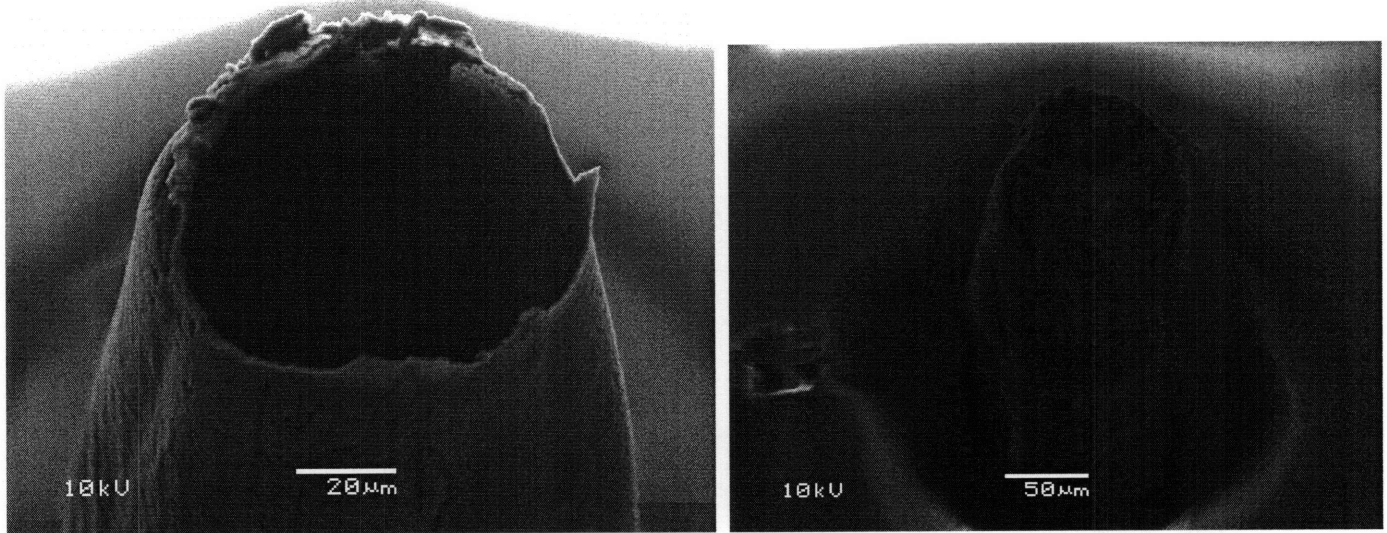


Figure 21. Depending on deposition parameters, either extremely thin shells or semi-filled pillars can be obtained.

While the theoretical basis for this phenomenon isn't clear, it may be related to pyrrole monomer depletion at the electrode surface for relatively low monomer bath concentrations combined high current densities, as well as surface effects (e.g. adsorption of nascent PPy chains onto the wall due to electrostatic interactions), which cause the polypyrrole to grow preferentially onto a substrate rather than vertically (Isaksson et al., 2007, Ludwig et al., 2006, Nyberg et al., 2007, Richardson-Burns et al., 2007, Xiao et al., 2006, Yang et al., 2005, Yang et al., 2007), (LaVan et al., 2003, Xiao et al., 2007). While monomer concentration and current possibly determine the ratio of growth along the surface of the mask as opposed to "straight up", deposition time is clearly of capital importance, as pillar thickness always increases with increased deposition time.

In addition to better characterizing this phenomenon, both theoretically and experimentally, and using TEM to get a better idea of the exact inner structure of the micropillars, it may be of interest testing this fabrication strategy with other conducting, biocompatible and biostable polymers, such as PEDOT (Isaksson et al., 2007, Ludwig et al., 2006, Nyberg et al., 2007, Richardson-Burns et al., 2007, Xiao et al., 2006, Yang et al., 2005, Yang et al., 2007).

A possible problem, especially with smaller, thinner electrode spikes would be their overgrowth by glial cells. A way to address this problem would be to switch the behavior of the micropillars from cell-repellant to cell adhesive after glial cell seeding and right before seeding the primary neurons. One possible embodiment of this idea would involve initially embedding hyaluronic acid (HA) in the PPy(Cen et al., 2004, Collier et al., 2000), seeding glial cells, culture them until they form a confluent monolayer, than add PLL or laminin which, being positively charged, would strongly bind to the negatively charged HA(Fukuda et al., 2006, Khademhosseini et al., 2004, Wright et al., 2007). Finally, the neurons would be seeded, and attach to the PLL/laminin-treated posts, as well as to the glial layer

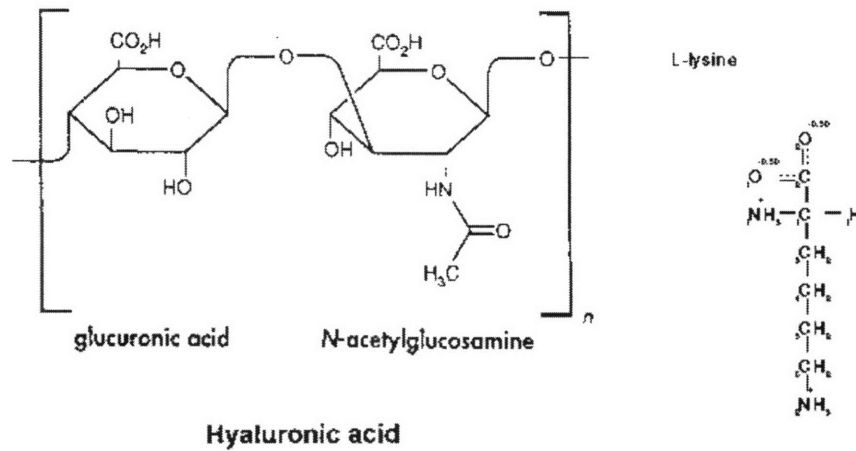
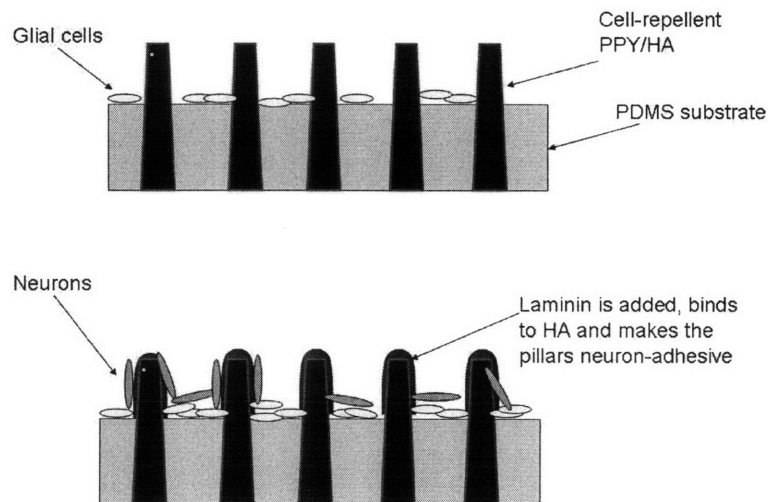


Figure 22. A. repeating unit of hyaluronic acid, www.chemistry.org B. L-lysine www.biocheminfo.org



3.2.4.3 Mask surface layer removal

After the PPy micropillars have been successfully grown, a surface layer of the mask needs to be removed in order to expose the top of the spikes. One way to do so would be to etch the masking material to the desired depth. While PDMS owes part of its wide use to its chemical stability, it can be etched in 1M Tetra-n-butylammonium fluoride (TBAF) in tetrahydrofuran (THF) while retaining sufficient mechanical stability.

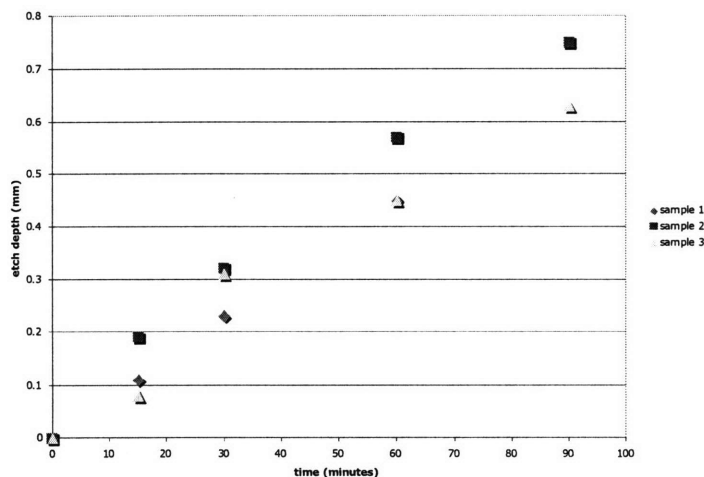


Figure 24. PDMS etch depth by 1M TBAF in THF versus time

Unfortunately, etching of PDMS tends to be unreliable, and reflow of molten material enveloping the spikes can be an issue. Another problem of etching is that some residual TBAF/THF can remain and poison cells. Other materials we tested, such as PMMA tended to have similar problems.

A much better approach was to use a PDMS/composite multilayered structure as the mask, and simply peel off the surface layers after deposition is complete. The PDMS self-adhesive properties ensure strong but reversible bonding between the different layers, so that the mask acts effectively as a monolithic unit during deposition, but the topmost layers can be rapidly removed afterwards.

While most of the work was carried out using bilayers of implant-grade PDMS (typically 250 μm thick), the same approach can be extended to trilayers, fabricated by sandwiching a thin glass coverslip between the two elastomer sheets, after plasma treating one side to ensure irreversible bonding to the bottom PDMS sheet.

The bottom polymer surface has the purpose of ensuring a tight seal between the mask and the glassy carbon or ITO electrode, constraining PPy growth in the desired pattern. It can be dispensed off, but at the cost of additional complexity in the deposition setup, where mechanical clamps or a vacuum can be used to the same effect, assuming perfect smoothness of the two surfaces to be brought in contact.

In fact, we have tested this idea by bonding a PDMS sacrificial layer on top of a 35 mm Falcon® culture dish, laser patterning it (from the reverse side), then clamping it onto a GC electrode for electrodeposition. Although the specific material employed was less than optimal (it doesn't get cut well on laser cutter, tends to get detached from PDMS, and culture dishes don't have a flat, featureless bottom), it did demonstrate the versatility of this approach.

Surface modification

As-received, PDMS is slightly hydrophobic (water contact angle $>80^\circ$). In order to render it hydrophilic, as well as to insure sterility, it can be plasma-treated after the PPy has been deposited. The plasma treatment, that can be effected in any standard asher employing oxygen or air plasma, oxidizes the surfaces, greatly improving their wettability with polar solvents, such as water.

Following plasma treatment the PDMS substrates can be coated with poly-L-lysine and/or laminin to improve cell adhesion. While in our current work the whole substrate was uniformly coated, an inkjet-like printing mechanism could be easily adapted for patterning adhesion molecules to help constrain network connectivity from the onset and complement activity-dependent plasticity, more closely mimicking the *in vivo* milieu

3.2.5 Current fabrication workflow

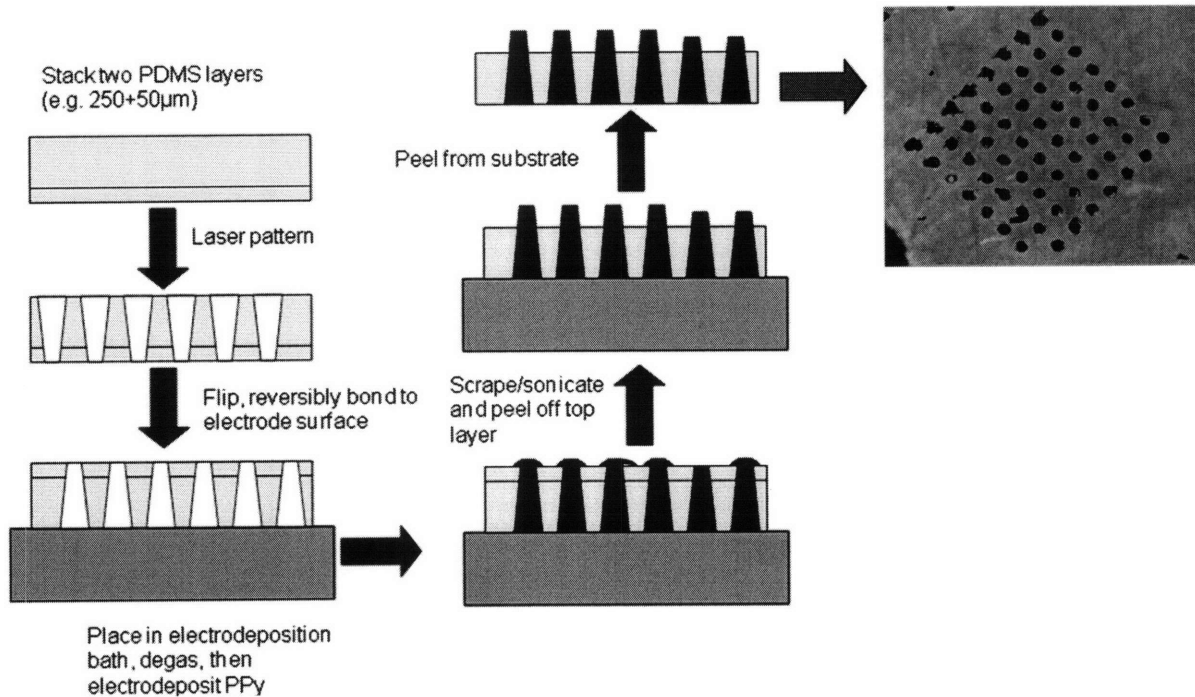


Figure 25. Workflow for making polypyrrole microelectrode arrays. Please refer to Appendix 2 for the detailed protocol.

3.2.6 Testing

Although virtually all of the work to date has gone into developing a novel fabrication method for the fabrication of all-polymer microelectrode arrays, in parallel we also started carrying out in vitro testing of the arrays. The main problem encountered was linked to the relative hydrophobicity of PDMS, as well as contamination issues. However, both were greatly ameliorated by introducing a plasma-cleaning step before cell culture, as well as by more careful cleaning and rinsing steps during fabrication to eliminate all traces of organic solvents and unpolymerized pyrrole.

Since this development came very late in time, we only tried cultures twice on treated substrates, getting neuronal growth and attachment for up to a week until, in one case, the substrates reverted to hydrophobic, possibly because of insufficient plasma treatment and laminin/PLL incubation, and, in the second case, the cultures got contaminated. Although the neurons growing on the PDMS tended to die after that time, glial cells tended to survive, despite the presence of specific growth inhibitors, normally used to produce “pure” neuronal cultures. Since the micropillars are optically opaque, it wasn’t possible to image cells growing onto them. However, neuronal cultures onto flat PPy/NaDBS and PPy/HA-coated ITO glasses showed good cell adhesion and survival.

In fact, the original purpose of the 3D geometry was to allow culturing of a glial monolayer, onto which to seed the primary neurons, and that now seems very feasible. In our tests, flat PPy substrates supported neuronal attachment and growth, and both glial cells and primary neurons are known from the literature to be able to attach and grow onto PDMS, as well as onto PPy. Further debugging the fabrication procedure and validating cell-viability for long-term cultures is, however, certainly the next step to take

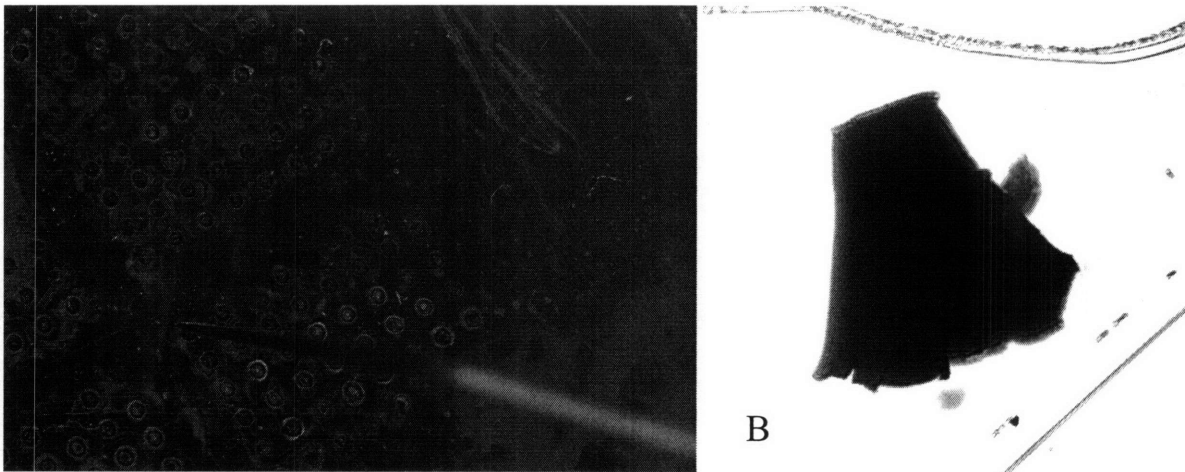


Figure 26 A. to test micropillar conductivity, one lead was connected to the glassy carbon substrate and the other, via a micromanipulated probe, to the PPy pillar, still embedded in the PDMS mask and attached to the substrate. **B.** One of the earliest micropillars, 250 μ m tall.

It would also be essential to characterize the electrical properties of the grown micropillars. Testing to date was carried out by measuring resistivity across individual

pillars, still attached to a GC substrate (see Fig.27A), yielding values of $\sim 1 \text{ k}\Omega$ for 500 μm pillars. An alternative approach would be to test the individual micropillars (see Fig. 27B) in the micro-fiber tester developed by Dr. Taberner, which would allow simultaneous measurement of electrical and mechanical properties.

3.2.7 Compatibility with standard cell-culture/high throughput formats

From the onset, we wanted our technology to be compatible with standard high-throughput formats. Laser-patterning technology suits admirably, so that proof-of-principle 8 by 8 by 96 arrays (see Fig. 28) have been patterned on a standard CO₂ laser in less than 3 minutes, and grown on glassy carbon crucibles in the same time it takes for a single array.

Using the excimer laser, 10 by 10 by 384 arrays can be quickly fabricated using mask-based techniques. If combined with beam-splitting, it should be possible to pattern an entire array (for 38,400 microspikes) in parallel, in a matter of minutes.

There is a variety of possible approaches to combining our flat substrates with standard cell-culture formats. Aside from laser-cutting holes in standard multi-well plates, then attaching them using a silicone adhesive to the membranes, as done for the first prototypes, possibly the simplest and best method would be to fabricate bottom-less PDMS well inserts (similar to regular multiwell plates, only without the bottom) in standard formats, then attaching them to the PMEA by plasma treating the two and overlaying them.

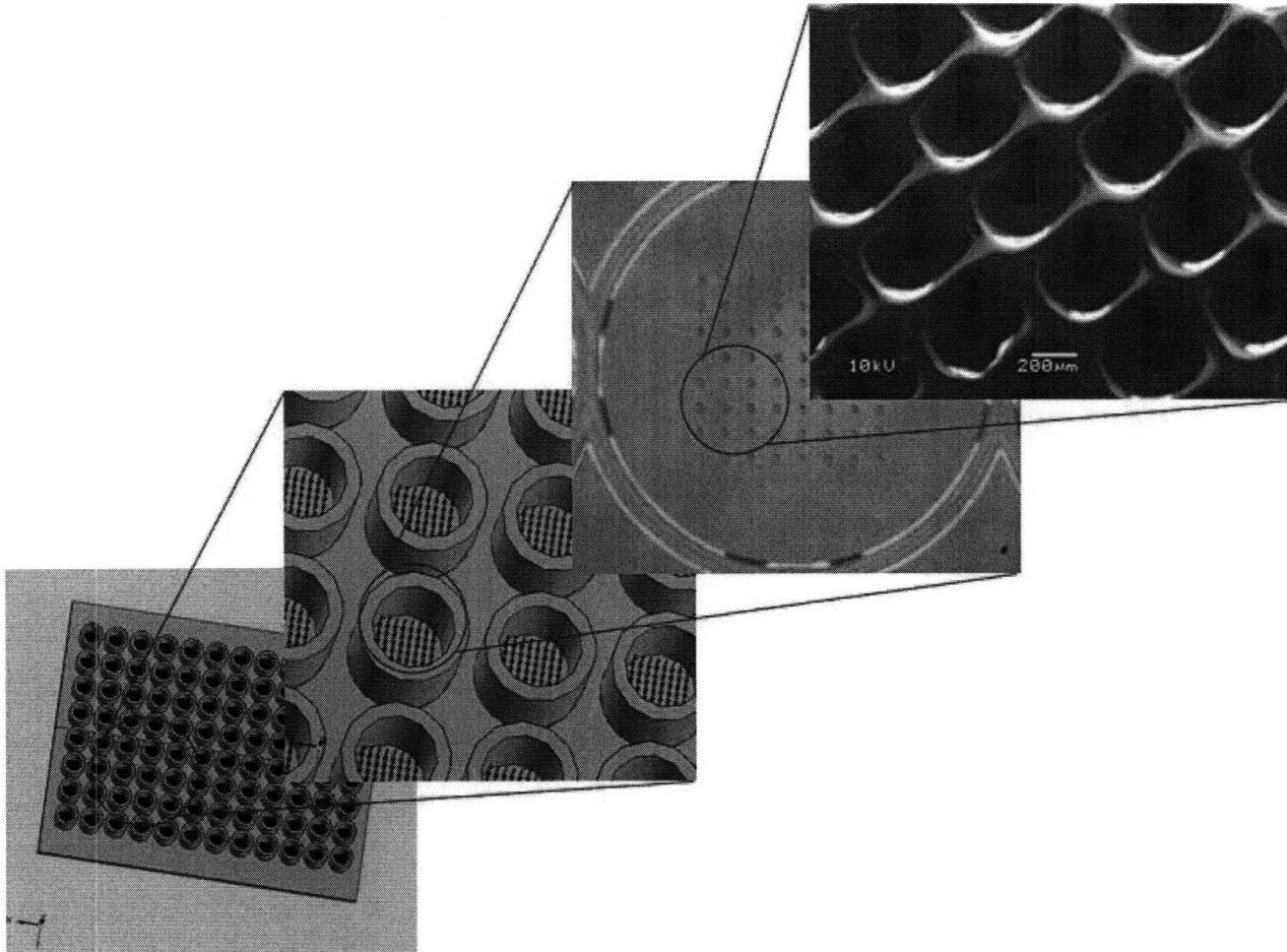


Figure 27. SolidEdge rendition of a 96 well with 8 by 8 electrode array at the bottom of the wells, single 8 by 8 subarray of the test 8 by 8 by 96 mask, and micropillars grown with a multi-array mask

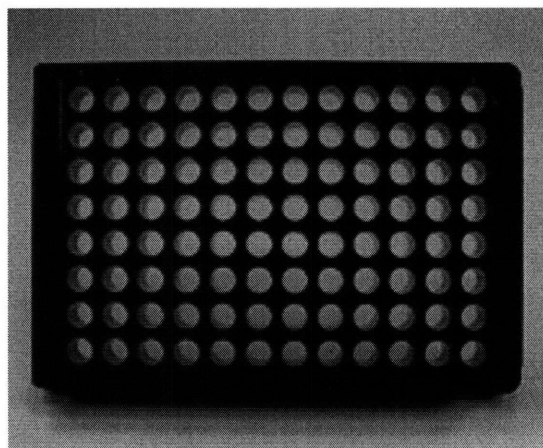


Figure 28. http://www.gracebio.com/Products/Microarraying/ProPlate_Plates/ something akin to the microtitre plate depicted above (without the patented sealing edges) could be fabricated and in PDMS and irreversibly bonded to the PMEAs by briefly plasma treating them both, the overlaying them and applying gentle pressure

4. CONCLUSIONS

4.1 What has been accomplished to date

We have developed a novel technology for the fabrication of disposable, all-polymer 3D microelectrode arrays, and developed a stimulator capable of individually addressing each microelectrode in a 64-electrodes array and operating in a software environment suitable for image capture and analysis. Finally, we have begun in vitro testing and validation of the suitability of the arrays for long-term neuronal culture.

4.2 Next steps for the PMEAs technology

The next steps will be, on one hand, full in vitro validation of the PMEAs as a suitable substrate for long-term glia/neurons coculture, on the other refining the fabrication techniques incorporating mask-based excimer laser micromachining techniques. The latter would allow us to manufacture extremely fine (10 to 25 μm) microelectrodes both in PDMS and in glass, and to machine large (e.g. 10 by 10 by 384) arrays in parallel.

After testing suitable techniques for fabricating large, fine-featured masks, it will be important to refine the electrodeposition setup to better be able to grow thousands or tens of thousands of electrodes in parallel.

Meanwhile, a better theoretical and experimental understanding of the formation of controlled-thickness microstructures should be pursued. A systematic exploration of the parameter space, finite element modeling and TEM imaging are likely to prove very useful approaches to this problem.

Finally, the fabrication method should be tested with other biocompatible conducting polymers, as well as polypyrroles doped with biologically active compounds, such as, for example, laminin-like peptide fragments.

4.3 Applications

In order to fully take advantage of the possibilities offered by the PMEAs technology, hardware capable of addressing multiwell 64-microelectrodes arrays should be developed, potentially using as a starting point the current stimulator.

While for initial testing simply connecting the existing camera to a microscope would be enough for trying calcium-dye imaging of neurons grown on the PMEAs, for future high-throughput applications a new setup will have to be engineered, as will image processing programs.

However, the current apparatus already appears suitable to study synaptic plasticity in a laboratory setting, and more particularly to start developing the idea of plasticity-driven network patterning in vitro, which would be in itself a major scientific accomplishment.

Appendix 1 Culture Protocol for CA3-CA1 neurons
From Margaret E Threadgil, PhD

Prepare coverslips by adding 50 μ l Matrigel (or PLL/laminin) per coverslip and leave in the incubator (overnight)

Warm up Plating medium in the incubator (lid should be open, better do it in the hood)

Prepare dishes with Hanks+20, ~3ml/dish. 3 dishes/one pup and an extra dish to wash.

Weigh out 20mg of Trypsin

Dissect in Hanks+20, cut CA3-CA1 in small chunks, then transfer to 15ml tube.

Wash 1-3 times with Hanks+20 (depends on the number of pups dissected)

Wash 3 times with Hanks salt solution to remove serum. Remove last wash.

Add 2.5ml Digestion solution +20 μ l Dnase + 20mg Trypsin (filter). Digest in the hood for 13min.

Wash 3 times with Hanks+20

Wash 3 times with Hanks salt solution, remove the last wash.

Add 2ml Dissociation solution +20 μ l Dnase

Triturate ~10 times with fire polished siliconized Pasteur Pipett

Wait for 3min in order to let larger clumps settle down

Transfer supernatant to a new tube and add 3ml Hanks+20. Centrifuge 10min at 4°C, 1000rpm

Aspirate Matrigel from coverslip completely (Matrigel seems to inhibit neuron growth)

Discard supernatant, dissolve pellet in plating medium, ~600 μ l/pup (2 hipp.), triturate 4, 5 times gently, plate 50 μ l/coverslip.

Leave in the incubator 1-2hr. (minimum 20min to let the cells attached). Add 1ml plating medium.

24-48 hr later, add 1ml medium with 4mM Ara-C (to inhibit glia growth)

Appendix 2: protocol for PMEA fabrication

Mask making:

- Design the desired pattern in Corel Draw, remembering to set the drawing parameters as no outlines, filled objects, minimum size (for CO₂ laser in lab) 75-100 μ m. If you try to go smaller you will still get features of approximately the same size, but less reliably. Of course using a different laser (e.g. excimer laser) would allow a reduction of almost two orders of magnitude in feature size
- Prepare the double layer PDMS membrane. If using two off-the-shelf implant-grade membranes, (e.g. 250 or 125 μ m) carefully peel off one side of paper backing, cut two sheets of the desired size, then carefully superimpose them, making sure that as they adhere to each other no air bubbles are trapped inside. A few drops of ethanol may help in the process.
- If outer PDMS layers as thin as 50 μ m are desired, it is possible to spin coat them, then adhere a 250 μ m sheet on top of it and remove the two together. Be aware that thin PDMS sheets are very fragile and hard to handle.
- Alternatively, a trilayer can be fabricated by having a thin (e.g. No.1) glass coverslip sandwiched between the two PDMS sheets. In that case, plasma treating the basement PDMS membrane is mandatory in order to assure strong bonding to the glass, while the outer (sacrificial) PDMS sheet must never be plasma treated, if not very briefly (a few seconds) since it has to be removed after PPy electrodeposition
- Place the PDMS bilayer on a flat piece of acrylic; it's better to remove the remaining paper backing at this point. Make sure the bilayer is laying flat and is stable on the substrate.
- Bring the laser head to the correct height using the focusing tool.
- The parameters have to be adjusted from time to time, depending both on the bilyer, on laser idiosyncrasies and on the desired tip width and taper angle. Good starting points for 250+250 μ m are Power 60-80%, Speed 3-5, resolution

1000dpi. It is best, however, to check a first test run under the 5X scope and adjust the parameters accordingly

Deposition:

- Clean the glassy carbon electrode: soap+water, ddH₂O, EtOH, acetone, EtOH, ddH₂O. Air dry, or dry under a nitrogen stream.
- Add a few drops of EtOH to the surface of the glassy carbon (which gives better results than ITO-coated glass) electrode, carefully position the mask (with the wider part facing the electrode surface) and smooth it, making sure there are no air bubbles left, nor any excess EtOH, for otherwise the mask will not bond well to the electrode.
- Leave to air dry for ~1hr, then place on a hot plate (50-70C) for >2hrs to dry out any residual ethanol
- In the meanwhile, prepare the deposition solution. Dissolve the desired dopant (NaDBS or HA, .1-.2M and 2mg/ml respectively) in ddH₂O, and stir until thoroughly dissolved.
- Add 0.1-0.2M pyrrole monomer (third cut) dropwise with a syringe, ideally bubbling nitrogen at the same time, to prevent oxidation. Leave to stir until ready for the deposition. It can also be prepared in advance, and stored at 4C, but after ~1-2 days the solution does appear to degrade.
- Clean and polish the copper counter-electrode (soap+ddh₂o, fine grained sandpaper, then cleaning as for electrode).
- Put the counterelectrode in the deposition chamber, making sure it fits snugly and flush with the wall. Lay the GC electrode with the mask on the bottom surface (mask facing up!), pour on the pyrrole/dopant solution and degas (under low vacuum, enough to get rid of most bubbles, but without having the mask detach)
- Move the GC electrode to the upright position, connect to the wires (see protocol on server for current setup), put in the temperature controlled chamber (25C) and start deposition.

- Current and deposition time control the thickness/morphology of the resulting pillars. Normal values are a current density of $\sim 20-40 \text{ A/m}^2$ (constant current), with a deposition duration of 3-5 hrs.

Surface treatment:

- After the deposition is complete, it should be enough to gently peel off the upper, sacrificial layer, to have the freestanding pillars.
- If some of the pillars get detached, it may help to gently scrape the top surface of the sacrificial layer to get rid of excess PPy that may have “crusted over” (also, reduce deposition time or change pyrrole monomer density/current density), and add a few drops of EtOH in between the two PDMS layer to help teasing them apart.
- Rinse the arrays with acetone, EtOH, ddH₂O (2x)
- Plasma-treat for $\sim 15''$ at full power (MTL asher, approximately the same on most other oxygen/air ashers), immediately cover with 100% or 70% ethanol to preserve both hydrophilicity and sterility.
- Leave for a few hrs in the hood, under 70% ethanol and UV until ready to coat.
- Aspirate ethanol, rinse 4x with sterile water, incubate overnight with laminin/Poly-L-lysine (1/10 mg/ml) solution. When ready to use, aspirate coating sln and rinse 2x with sterile water. Seed cells at high concentration (as high as possible) in as small a drop of plating medium as possible. After 30'-1hr add the rest of the plating medium.

REFERENCES

- ABBOTT, L. F. & NELSON, S. B. (2000) Synaptic plasticity: taming the beast. *Nat Neurosci*, 3 Suppl, 1178-83.
- BA BOLTO, R. M. A. D. W. (1963) Electronic Conduction in Polymers. III. Electronic Properties of Polypyrrole. *Australian Journal of Chemistry*, 16, 1090-1103.
- BALIMANE, P. V. & CHONG, S. (2005) Cell culture-based models for intestinal permeability: a critique. *Drug Discov Today*, 10, 335-43.
- BARTH, A. L. & MALENKA, R. C. (2001) NMDAR EPSC kinetics do not regulate the critical period for LTP at thalamocortical synapses. *Nat Neurosci*, 4, 235-6.
- BEOM JUN, S., HYND, M., DOWELL-MESFIN, N., SMITH, K., TURNER, J., SHAIN, W. & JUNE KIM, S. (2005) Synaptic Connectivity of a Low Density Patterned Neuronal Network Produced on the Poly-L-Lysine Stamped Microelectrode Array. *Conf Proc IEEE Eng Med Biol Soc*, 7, 7604-7607.
- BI, G. & POO, M. (2001) Synaptic modification by correlated activity: Hebb's postulate revisited. *Annu Rev Neurosci*, 24, 139-66.
- BI, G. Q. & POO, M. M. (1998) Synaptic modifications in cultured hippocampal neurons: dependence on spike timing, synaptic strength, and postsynaptic cell type. *J Neurosci*, 18, 10464-72.
- BOATENG, S. Y., HARTMAN, T. J., AHLUWALIA, N., VIDULA, H., DESAI, T. A. & RUSSELL, B. (2003) Inhibition of fibroblast proliferation in cardiac myocyte cultures by surface microtopography. *Am J Physiol Cell Physiol*, 285, C171-82.
- BOETTIGER, C. A. & DOUPE, A. J. (2001) Developmentally restricted synaptic plasticity in a songbird nucleus required for song learning. *Neuron*, 31, 809-18.
- BRECKENRIDGE, L. J., WILSON, R. J., CONNOLLY, P., CURTIS, A. S., DOW, J. A., BLACKSHAW, S. E. & WILKINSON, C. D. (1995) Advantages of using microfabricated extracellular electrodes for in vitro neuronal recording. *J Neurosci Res*, 42, 266-76.
- BROACH, J. R. & THORNER, J. (1996) High-throughput screening for drug discovery. *Nature*, 384, 14-6.
- BUCHS, N. J. & SENN, W. (2002) Spike-based synaptic plasticity and the emergence of direction selective simple cells: simulation results. *J Comput Neurosci*, 13, 167-86.
- CARSWELL, A. D., O'REAR, E. A. & GRADY, B. P. (2003) Adsorbed surfactants as templates for the synthesis of morphologically controlled polyaniline and polypyrrole nanostructures on flat surfaces: from spheres to wires to flat films. *J Am Chem Soc*, 125, 14793-800.
- CASTEL, D., PITAVAL, A., DEBILY, M. A. & GIDROL, X. (2006) Cell microarrays in drug discovery. *Drug Discov Today*, 11, 616-22.
- CEN, L., NEOH, K. G., LI, Y. & KANG, E. T. (2004) Assessment of in vitro bioactivity of hyaluronic acid and sulfated hyaluronic acid functionalized electroactive polymer. *Biomacromolecules*, 5, 2238-46.

- CLAVEROL-TINTURE, E., CABESTANY, J. & ROSELL, X. (2007) Multisite recording of extracellular potentials produced by microchannel-confined neurons in-vitro. *IEEE Trans Biomed Eng*, 54, 331-5.
- CLAVEROL-TINTURE, E., GHIRARDI, M., FIUMARA, F., ROSELL, X. & CABESTANY, J. (2005) Multielectrode arrays with elastomeric microstructured overlays for extracellular recordings from patterned neurons. *J Neural Eng*, 2, L1-7.
- COLLIER, J. H., CAMP, J. P., HUDSON, T. W. & SCHMIDT, C. E. (2000) Synthesis and characterization of polypyrrole-hyaluronic acid composite biomaterials for tissue engineering applications. *J Biomed Mater Res*, 50, 574-84.
- CONSTANTINE-PATON, M. (2006) Shining light on spike timing-dependent plasticity. *Neuron*, 50, 5-7.
- CUI, X., WILER, J., DZAMAN, M., ALTSCHULER, R. A. & MARTIN, D. C. (2003) In vivo studies of polypyrrole/peptide coated neural probes. *Biomaterials*, 24, 777-87.
- DAN, Y. & POO, M. M. (2004) Spike timing-dependent plasticity of neural circuits. *Neuron*, 44, 23-30.
- DAN, Y. & POO, M. M. (2006) Spike timing-dependent plasticity: from synapse to perception. *Physiol Rev*, 86, 1033-48.
- FLEMMING, R. G., MURPHY, C. J., ABRAMS, G. A., GOODMAN, S. L. & NEALEY, P. F. (1999) Effects of synthetic micro- and nano-structured surfaces on cell behavior. *Biomaterials*, 20, 573-88.
- FOFONOFF, T. A., MARTEL, S. M., HATSOPOULOS, N. G., DONOGHUE, J. P. & HUNTER, I. W. (2004) Microelectrode array fabrication by electrical discharge machining and chemical etching. *IEEE Trans Biomed Eng*, 51, 890-5.
- FUKUDA, J., KHADEMHOSEINI, A., YEH, J., ENG, G., CHENG, J., FAROKHZAD, O. C. & LANGER, R. (2006) Micropatterned cell co-cultures using layer-by-layer deposition of extracellular matrix components. *Biomaterials*, 27, 1479-86.
- GEORGE, P. M., LYCKMAN, A. W., LAVAN, D. A., HEGDE, A., LEUNG, Y., AVASARE, R., TESTA, C., ALEXANDER, P. M., LANGER, R. & SUR, M. (2005) Fabrication and biocompatibility of polypyrrole implants suitable for neural prosthetics. *Biomaterials*, 26, 3511-9.
- GOMEZ, N. & SCHMIDT, C. E. (2007) Nerve growth factor-immobilized polypyrrole: bioactive electrically conducting polymer for enhanced neurite extension. *J Biomed Mater Res A*, 81, 135-49.
- HUSH, N. S. (2003) An Overview of the First Half-Century of Molecular Electronics. *Ann. N.Y. Acad. Sci.*, 1-20.
- ISAKSSON, J., KJALL, P., NILSSON, D., ROBINSON, N. D., BERGGREN, M. & RICHTER-DAHLFORS, A. (2007) Electronic control of Ca²⁺ signalling in neuronal cells using an organic electronic ion pump. *Nat Mater*, 6, 673-9.
- ISEKI, M., SAITO, K., KUHARA, K. & MIZUKAMI, A. (1991) Electrochemical Exchange Process of Dopant Anions in Polypyrrole. *Synthetic Metals*, 40, 117-126.
- JAMES, C. D., DAVIS, R., MEYER, M., TURNER, A., TURNER, S., WITHERS, G., KAM, L., BANKER, G., CRAIGHEAD, H., ISAACSON, M., TURNER, J. & SHAIN, W. (2000) Aligned microcontact printing of micrometer-scale poly-L-

- lysine structures for controlled growth of cultured neurons on planar microelectrode arrays. *IEEE Trans Biomed Eng*, 47, 17-21.
- JAMES, C. D., SPENCE, A. J., DOWELL-MESFIN, N. M., HUSSAIN, R. J., SMITH, K. L., CRAIGHEAD, H. G., ISAACSON, M. S., SHAIN, W. & TURNER, J. N. (2004) Extracellular recordings from patterned neuronal networks using planar microelectrode arrays. *IEEE Trans Biomed Eng*, 51, 1640-8.
- JIMBO, Y., ROBINSON, H. P. & KAWANA, A. (1993) Simultaneous measurement of intracellular calcium and electrical activity from patterned neural networks in culture. *IEEE Trans Biomed Eng*, 40, 804-10.
- JUN, S. B., HYND, M. R., DOWELL-MESFIN, N., SMITH, K. L., TURNER, J. N., SHAIN, W. & KIM, S. J. (2007) Low-density neuronal networks cultured using patterned poly-l-lysine on microelectrode arrays. *J Neurosci Methods*, 160, 317-26.
- KANATZIDIS, M. G. (1990) Conductive Polymers. *Chemical & Engineering News*, 68, 36-&.
- KEOHAN, F., WEI, X. F., WONGSARNPIGOON, A., LAZARO, E., DARGA, J. E. & GRILL, W. M. (2007) Fabrication and evaluation of conductive elastomer electrodes for neural stimulation. *J Biomater Sci Polym Ed*, 18, 1057-73.
- KHADEMHOSEINI, A., SUH, K. Y., YANG, J. M., ENG, G., YEH, J., LEVENBERG, S. & LANGER, R. (2004) Layer-by-layer deposition of hyaluronic acid and poly-L-lysine for patterned cell co-cultures. *Biomaterials*, 25, 3583-92.
- KIM, D. H., ABIDIAN, M. & MARTIN, D. C. (2004) Conducting polymers grown in hydrogel scaffolds coated on neural prosthetic devices. *J Biomed Mater Res A*, 71, 577-85.
- KOTWAL, A. & SCHMIDT, C. E. (2001) Electrical stimulation alters protein adsorption and nerve cell interactions with electrically conducting biomaterials. *Biomaterials*, 22, 1055-64.
- LAVAN, D. A., GEORGE, P. M. & LANGER, R. (2003) Simple, three-dimensional microfabrication of electrodeposited structures. *Angewandte Chemie-International Edition*, 42, 1262-1265.
- LENG, T., WU, P., MEHENTI, N. Z., BENT, S. F., MARMOR, M. F., BLUMENKRANZ, M. S. & FISHMAN, H. A. (2004) Directed retinal nerve cell growth for use in a retinal prosthesis interface. *Invest Ophthalmol Vis Sci*, 45, 4132-7.
- LUDWIG, K. A., URAM, J. D., YANG, J., MARTIN, D. C. & KIPKE, D. R. (2006) Chronic neural recordings using silicon microelectrode arrays electrochemically deposited with a poly(3,4-ethylenedioxythiophene) (PEDOT) film. *J Neural Eng*, 3, 59-70.
- MARKRAM, H., LUBKE, J., FROTSCHER, M., ROTH, A. & SAKMANN, B. (1997) Physiology and anatomy of synaptic connections between thick tufted pyramidal neurones in the developing rat neocortex. *J Physiol*, 500 (Pt 2), 409-40.
- NISHIYAMA, M., HONG, K., MIKOSHIBA, K., POO, M. M. & KATO, K. (2000) Calcium stores regulate the polarity and input specificity of synaptic modification. *Nature*, 408, 584-8.

- NYBERG, T., SHIMADA, A. & TORIMITSU, K. (2007) Ion conducting polymer microelectrodes for interfacing with neural networks. *J Neurosci Methods*, 160, 16-25.
- ORRY, A. J., ABAGYAN, R. A. & CAVASOTTO, C. N. (2006) Structure-based development of target-specific compound libraries. *Drug Discov Today*, 11, 261-6.
- R MCNEILL, R. S., JH WARDLAW AND DE WEISS (1963) Electronic Conduction in Polymers. I. The Chemical Structure of Polypyrrole. *Australian Journal of Chemistry*, 16, 1056-1075.
- RICHARDSON-BURNS, S. M., HENDRICKS, J. L., FOSTER, B., POVLIICH, L. K., KIM, D. H. & MARTIN, D. C. (2007) Polymerization of the conducting polymer poly(3,4-ethylenedioxythiophene) (PEDOT) around living neural cells. *Biomaterials*, 28, 1539-52.
- ROLSTON, J. D., WAGENAAR, D. A. & POTTER, S. M. (2007) Precisely timed spatiotemporal patterns of neural activity in dissociated cortical cultures. *Neuroscience*, 148, 294-303.
- SCHMIDT, C. E., SHASTRI, V. R., VACANTI, J. P. & LANGER, R. (1997) Stimulation of neurite outgrowth using an electrically conducting polymer. *Proc Natl Acad Sci U S A*, 94, 8948-53.
- SHI, G., ROUABHIA, M., WANG, Z., DAO, L. H. & ZHANG, Z. (2004) A novel electrically conductive and biodegradable composite made of polypyrrole nanoparticles and polylactide. *Biomaterials*, 25, 2477-88.
- SJOSTROM, P. J., TURRIGIANO, G. G. & NELSON, S. B. (2003) Neocortical LTD via coincident activation of presynaptic NMDA and cannabinoid receptors. *Neuron*, 39, 641-54.
- SONG, H. K., TOSTE, B., AHMANN, K., HOFFMAN-KIM, D. & PALMORE, G. T. (2006) Micropatterns of positive guidance cues anchored to polypyrrole doped with polyglutamic acid: a new platform for characterizing neurite extension in complex environments. *Biomaterials*, 27, 473-84.
- SONG, S. & ABBOTT, L. F. (2001) Cortical development and remapping through spike timing-dependent plasticity. *Neuron*, 32, 339-50.
- SONG, S., MILLER, K. D. & ABBOTT, L. F. (2000) Competitive Hebbian learning through spike-timing-dependent synaptic plasticity. *Nat Neurosci*, 3, 919-26.
- STAUFFER, W. R. & CUI, X. T. (2006) Polypyrrole doped with 2 peptide sequences from laminin. *Biomaterials*, 27, 2405-13.
- TOOKER, A., MENG, E., ERICKSON, J., TAI, Y. C. & PINE, J. (2005) Biocompatible parylene neurocages. Developing a robust method for live neural network studies. *IEEE Eng Med Biol Mag*, 24, 30-3.
- WADHWA, R., LAGENAUR, C. F. & CUI, X. T. (2006) Electrochemically controlled release of dexamethasone from conducting polymer polypyrrole coated electrode. *J Control Release*, 110, 531-41.
- WAGENAAR, D. A., NADASDY, Z. & POTTER, S. M. (2006a) Persistent dynamic attractors in activity patterns of cultured neuronal networks. *Phys Rev E Stat Nonlin Soft Matter Phys*, 73, 051907.

- WAGENAAR, D. A., PINE, J. & POTTER, S. M. (2006b) An extremely rich repertoire of bursting patterns during the development of cortical cultures. *BMC Neurosci*, 7, 11.
- WAGENAAR, D. A., PINE, J. & POTTER, S. M. (2006c) Searching for plasticity in dissociated cortical cultures on multi-electrode arrays. *J Negat Results Biomed*, 5, 16.
- WAGENAAR, D. A. & POTTER, S. M. (2002) Real-time multi-channel stimulus artifact suppression by local curve fitting. *J Neurosci Methods*, 120, 113-20.
- WANG, X., GU, X., YUAN, C., CHEN, S., ZHANG, P., ZHANG, T., YAO, J., CHEN, F. & CHEN, G. (2004a) Evaluation of biocompatibility of polypyrrole in vitro and in vivo. *J Biomed Mater Res A*, 68, 411-22.
- WANG, Z., ROBERGE, C., DAO, L. H., WAN, Y., SHI, G., ROUABHIA, M., GUIDOIN, R. & ZHANG, Z. (2004b) In vivo evaluation of a novel electrically conductive polypyrrole/poly(D,L-lactide) composite and polypyrrole-coated poly(D,L-lactide-co-glycolide) membranes. *J Biomed Mater Res A*, 70, 28-38.
- WANG, Z., ROBERGE, C., WAN, Y., DAO, L. H., GUIDOIN, R. & ZHANG, Z. (2003) A biodegradable electrical bioconductor made of polypyrrole nanoparticle/poly(D,L-lactide) composite: A preliminary in vitro biostability study. *J Biomed Mater Res A*, 66, 738-46.
- WONG, J. Y., LANGER, R. & INGBER, D. E. (1994) Electrically conducting polymers can noninvasively control the shape and growth of mammalian cells. *Proc Natl Acad Sci U S A*, 91, 3201-4.
- WRIGHT, D., RAJALINGAM, B., SELVARASAH, S., DOKMECI, M. R. & KHADEMOSSEINI, A. (2007) Generation of static and dynamic patterned co-cultures using microfabricated parylene-C stencils. *Lab Chip*, 7, 1272-9.
- WU, G. & DOBERSTEIN, S. K. (2006) HTS technologies in biopharmaceutical discovery. *Drug Discov Today*, 11, 718-24.
- XIAO, R., CHO, S. I., LIU, R. & LEE, S. B. (2007) Controlled electrochemical synthesis of conductive polymer nanotube structures. *J Am Chem Soc*, 129, 4483-9.
- XIAO, Y., MARTIN, D. C., CUI, X. & SHENAI, M. (2006) Surface modification of neural probes with conducting polymer poly(hydroxymethylated-3,4-ethylenedioxythiophene) and its biocompatibility. *Appl Biochem Biotechnol*, 128, 117-30.
- YANG, J., KIM, D. H., HENDRICKS, J. L., LEACH, M., NORTHEY, R. & MARTIN, D. C. (2005) Ordered surfactant-templated poly(3,4-ethylenedioxythiophene) (PEDOT) conducting polymer on microfabricated neural probes. *Acta Biomater*, 1, 125-36.
- YANG, J., LIPKIN, K. & MARTIN, D. C. (2007) Electrochemical fabrication of conducting polymer poly(3,4-ethylenedioxythiophene) (PEDOT) nanofibrils on microfabricated neural prosthetic devices. *J Biomater Sci Polym Ed*, 18, 1075-89.
- ZAKHARENKO, S. S., ZABLOW, L. & SIEGELBAUM, S. A. (2001) Visualization of changes in presynaptic function during long-term synaptic plasticity. *Nat Neurosci*, 4, 711-7.
- ZHANG, L. I., TAO, H. W., HOLT, C. E., HARRIS, W. A. & POO, M. (1998) A critical window for cooperation and competition among developing retinotectal synapses. *Nature*, 395, 37-44.

- ZHANG, W. & LINDEN, D. J. (2003) The other side of the engram: experience-driven changes in neuronal intrinsic excitability. *Nat Rev Neurosci*, 4, 885-900.
- ZHANG, Z., ROUABHIA, M., WANG, Z., ROBERGE, C., SHI, G., ROCHE, P., LI, J. & DAO, L. H. (2007) Electrically conductive biodegradable polymer composite for nerve regeneration: electricity-stimulated neurite outgrowth and axon regeneration. *Artif Organs*, 31, 13-22.